Supramolecular Control over Pillararene-based LCST Phase Behaviour

Li Wang,[a] Xing Li,[a] Qiao Zhang,[a] Zheng Luo,[a] Yan Deng,[a] Wen Yang,[a] Shengyi Dong,[a]* Qiu-an Wang,[a]* Chengyou Han[b]*

[a]*College of Chemistry and Chemical Engineering, Hunan University, Changsha 410082, Hunan, P. R. China. E-mail: dongsy@hnu.edu.cn, WangQA@hnu.edu.cn*

[b]*Dpartment of Chemistry, College of Science, China University of Petroleum (East China), Qingdao, 266580. E-mail: hanchengyou@upc.edu.cn.*

Electronic Supplementary Information

Table of Contents

1. Materials and methods

Materials. All reagents were commercially available and used as supplied without further purification. **P5** was synthesized according to reported methods.[S1]

Measurements. All the 2D NOESY, variable temperature ^{1}H NMR and ^{1}H NMR spectra were collected on a Bruker Ascend TM 400MHz spectrometer. The transmittance experiments were measured at 550 nm using a Lambda 950 UV/Vis/NIR spectrometer with a temperature controllable system. The heating rate was adjusted at 1.0 °C min $^{-1}$. Unless otherwise stated, samples were dissolved in Milli-Q water. MALDI-TOF mass spectrometry was performed on a Shimadzu Biotech AXIMA Performance instrument.

2. ^{1}H NMR spectra of equimolar mixture of **P5** and **G1** in D_2O

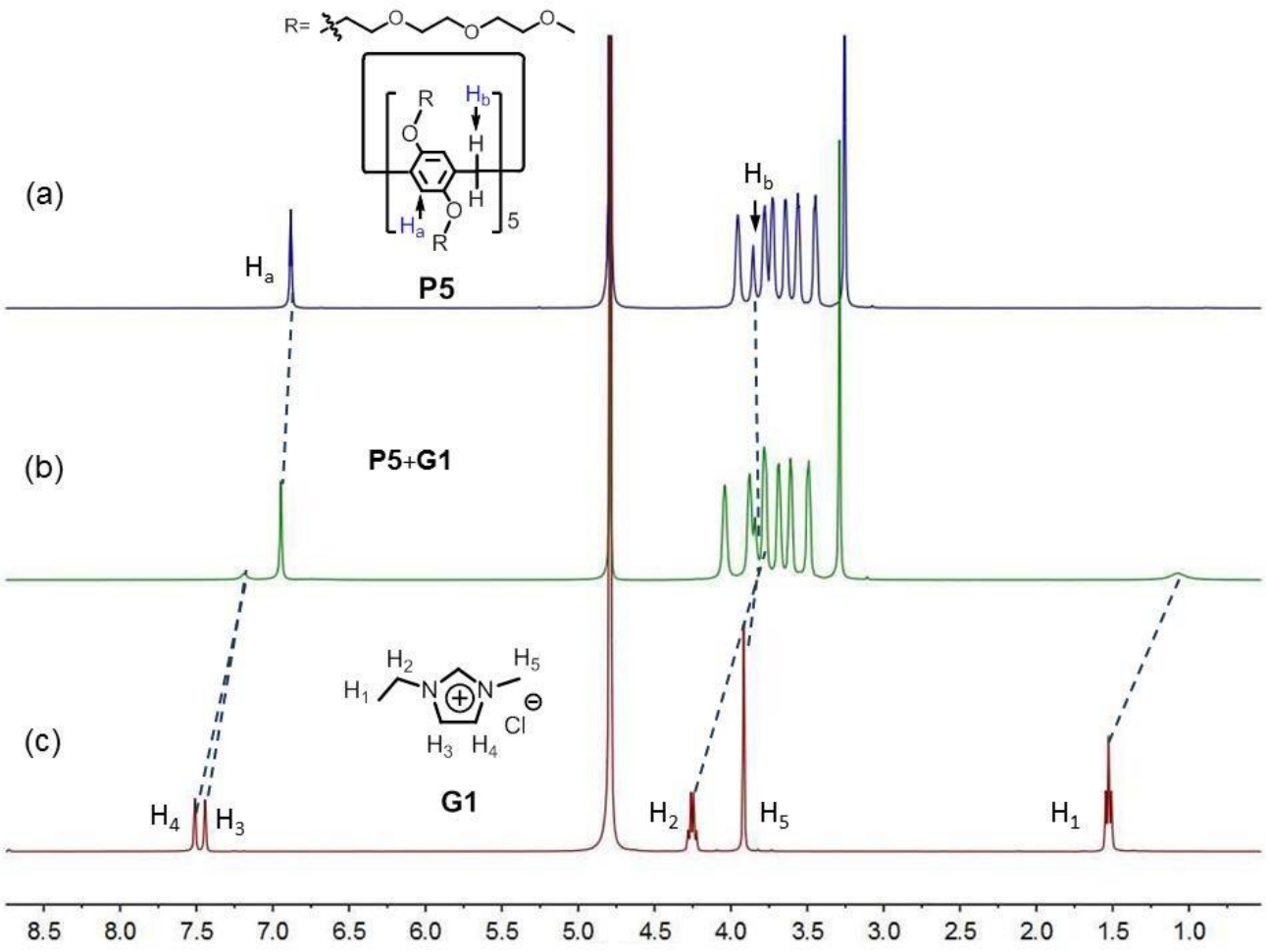

Figure S1. ^{1}H NMR spectra (400 MHz, D_2O, room temperature) of: (a) **P5** (2.00 mM); (b) **P5** (2.00 mM) and **G1** (2.00 mM); (c) **G1** (2.00 mM).

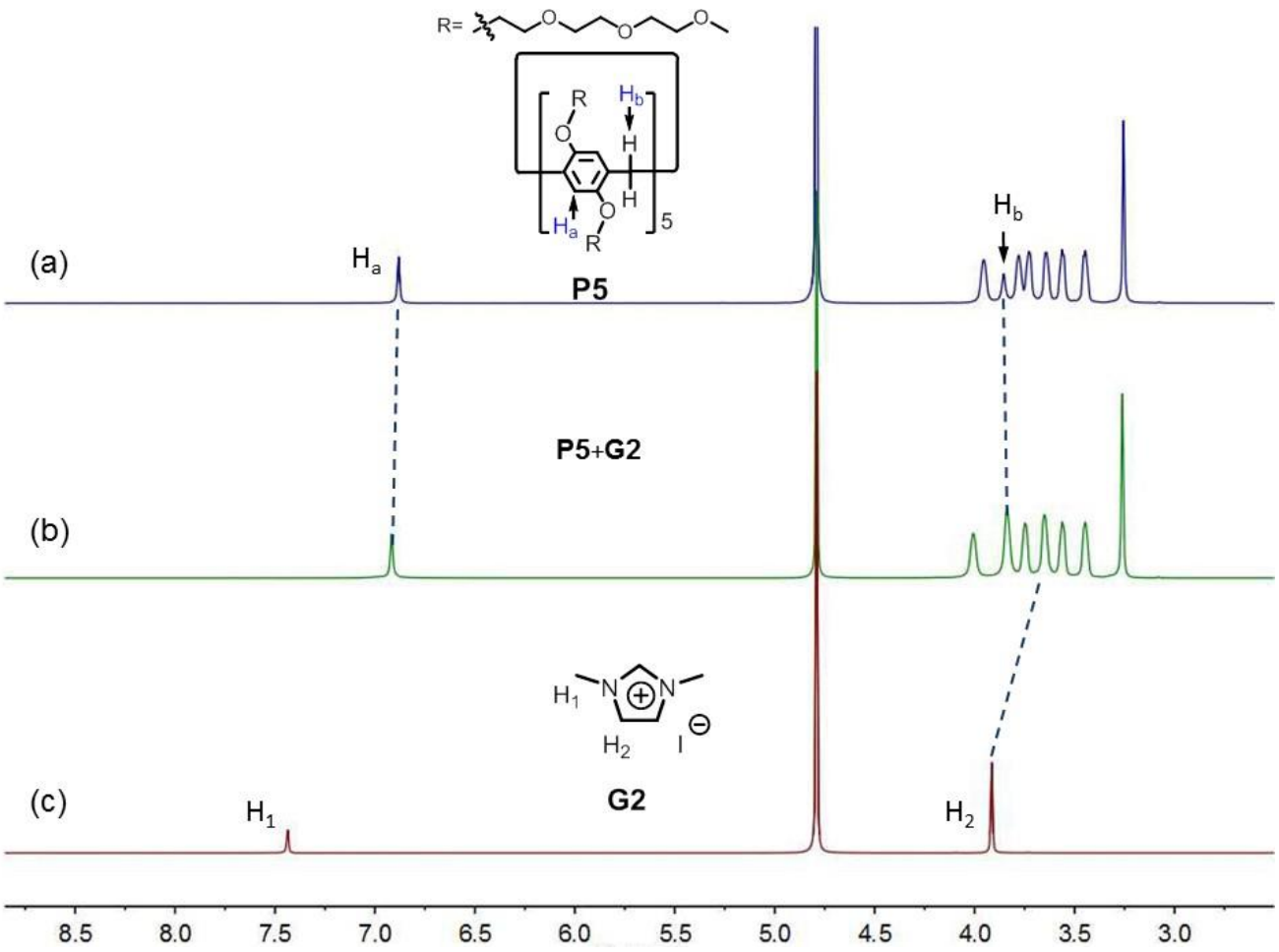

Figure S2. ^{1}H NMR spectra (400 MHz, D_2O, room temperature) of: (a) **P5** (2.00 mM); (b) **P5** (2.00 mM) and **G2** (2.00 mM); (c) **G2** (2.00 mM).

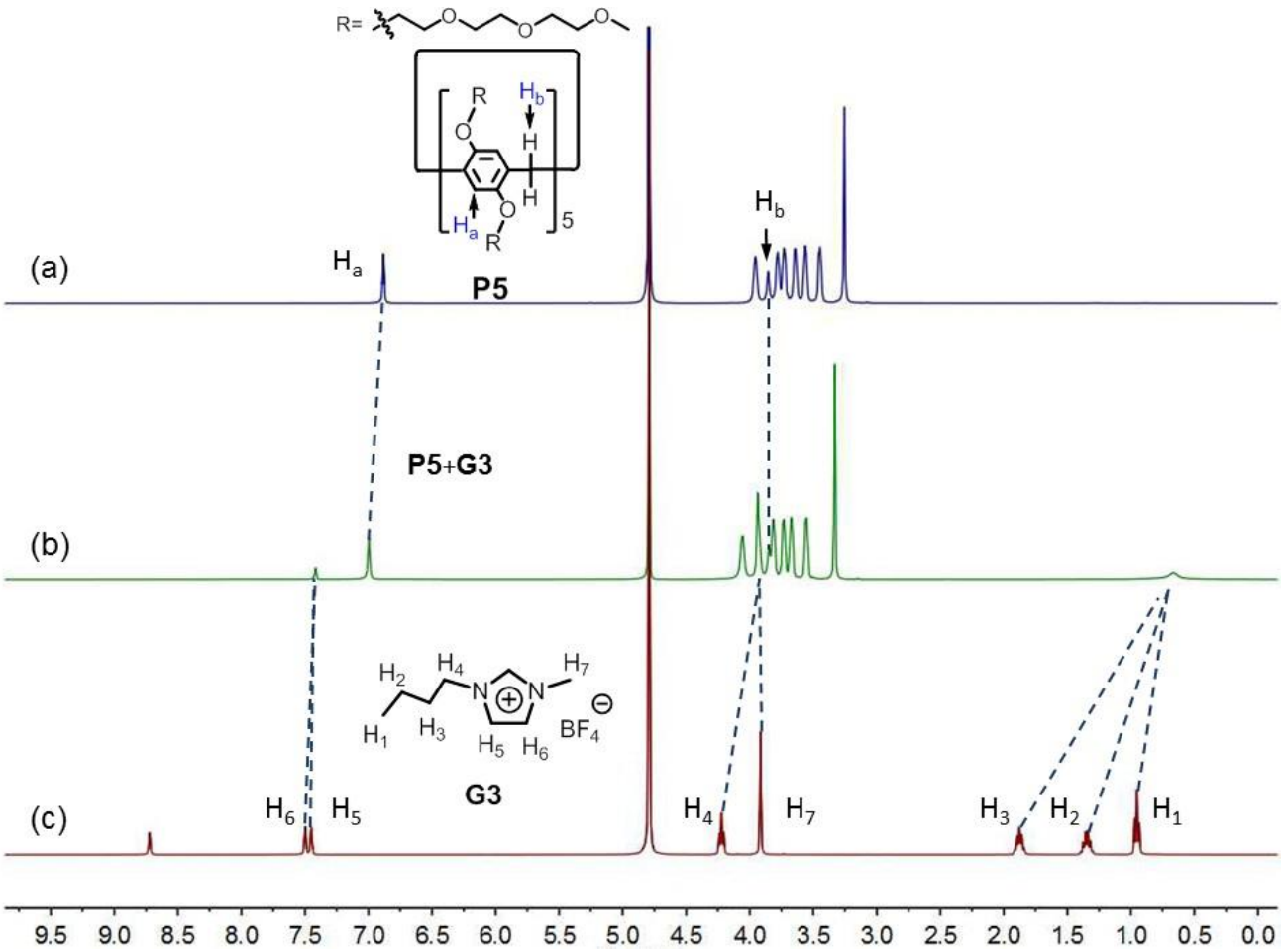

Figure S3. ^{1}H NMR spectra (400 MHz, D_2O, room temperature) of: (a) **P5** (2.00 mM); (b) **P5** (2.00 mM) and **G3** (2.00 mM); (c) **G3** (2.00 mM).

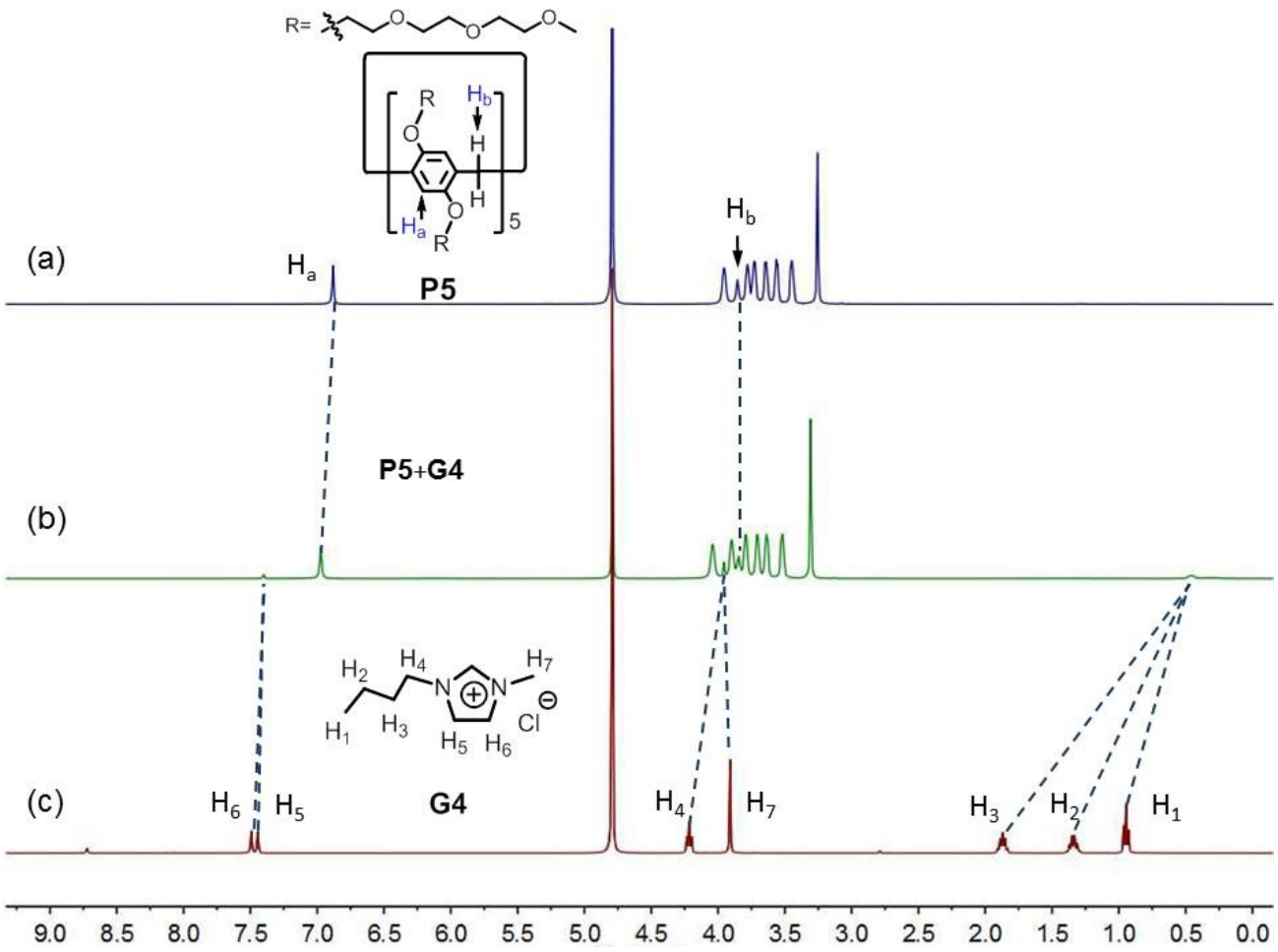

Figure S4. ^{1}H NMR spectra (400 MHz, D_2O, room temperature) of: (a) **P5** (2.00 mM); (b) **P5** (2.00 mM) and **G4** (2.00 mM); (c) **G4** (2.00 mM).

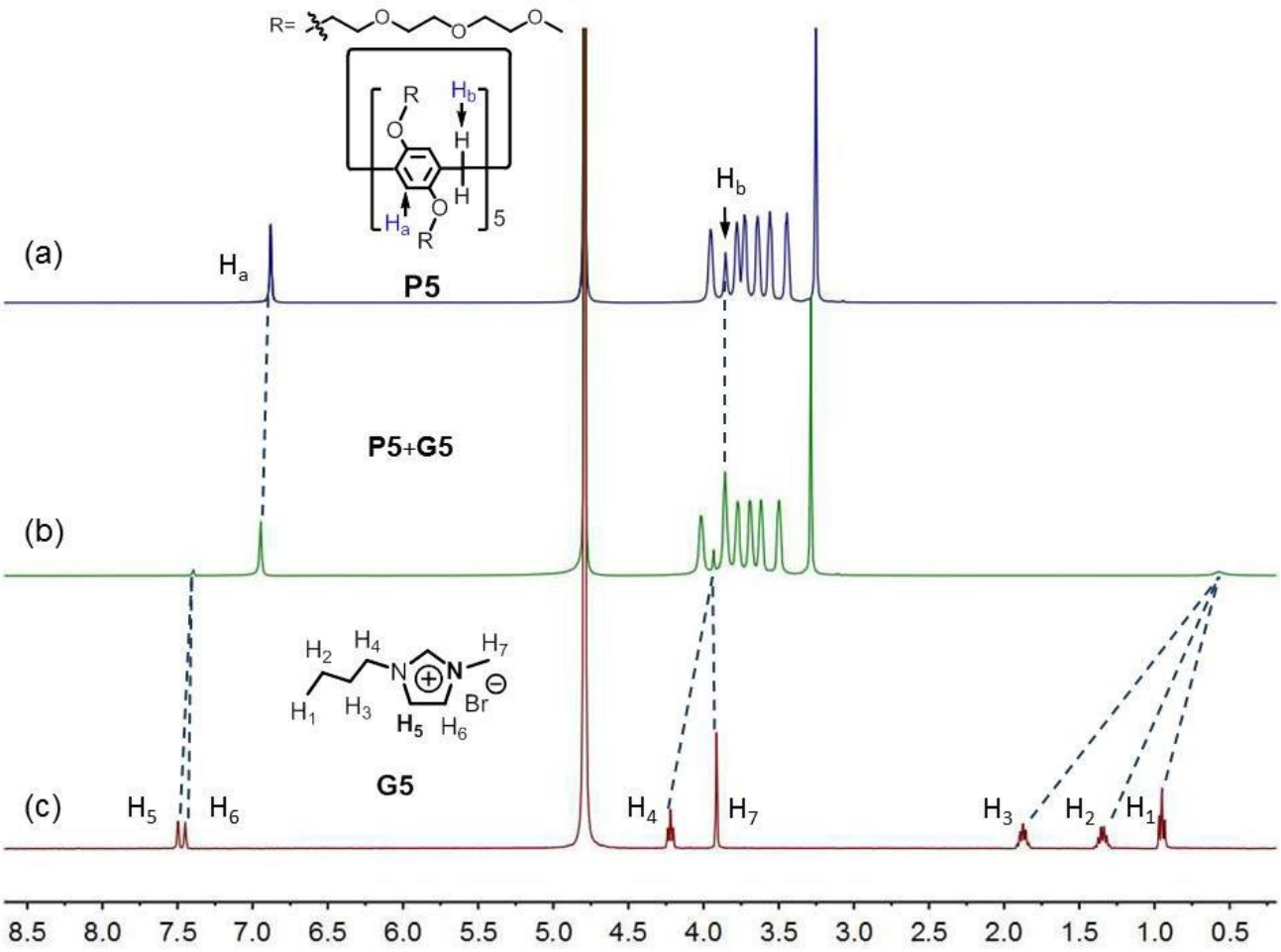

Figure S5. ^{1}H NMR spectra (400 MHz, D_2O, room temperature) of: (a) **P5** (2.00 mM); (b) **P5** (2.00 mM) and **G5** (2.00 mM); (c) **G5** (2.00 mM).

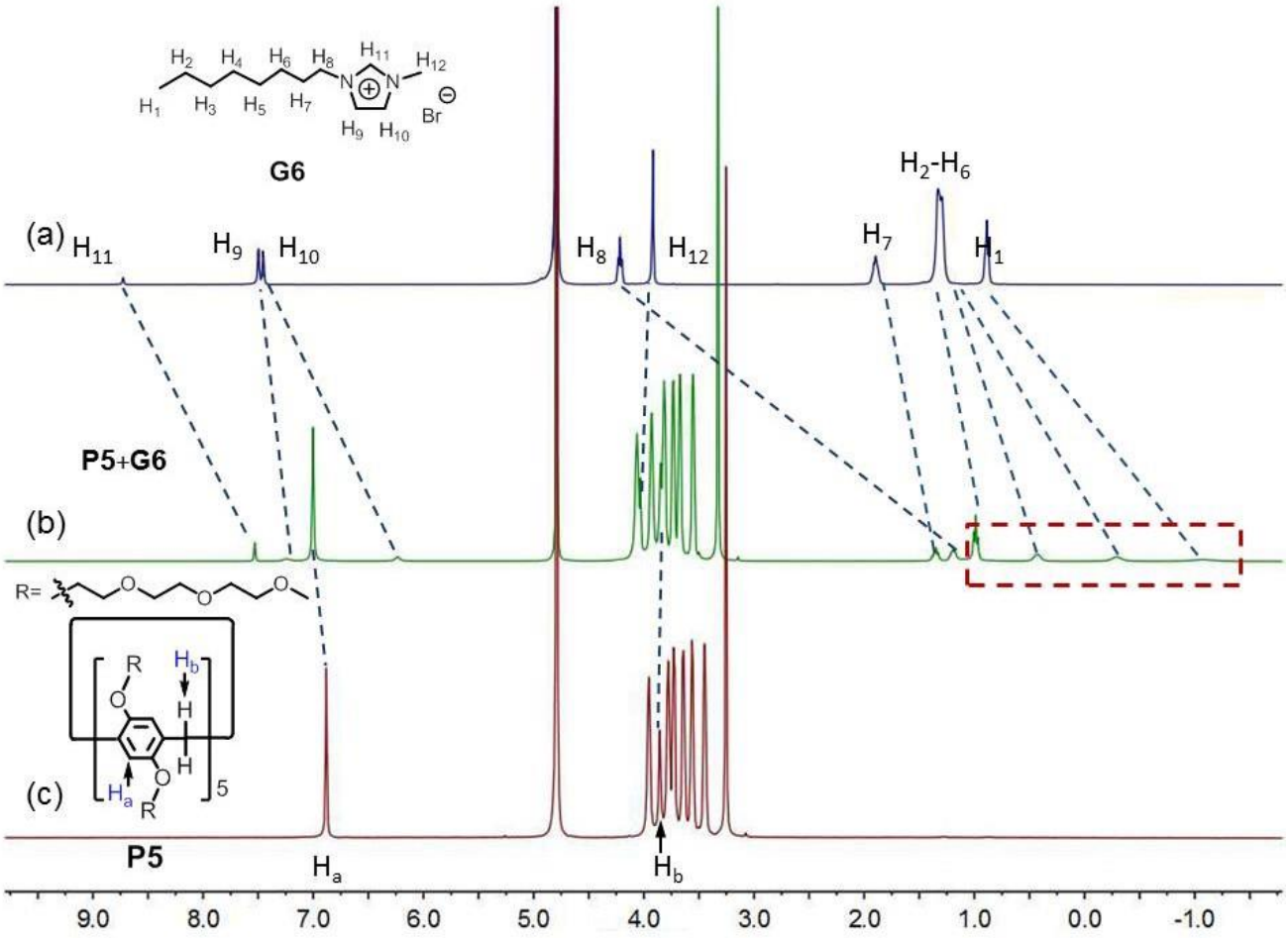

Figure S6. ^{1}H NMR spectra (400 MHz, D_2O, room temperature) of: (a) **P5** (2.00 mM); (b) **P5** (2.00 mM) and **G6** (2.00 mM); (c) **G6** (2.00 mM).

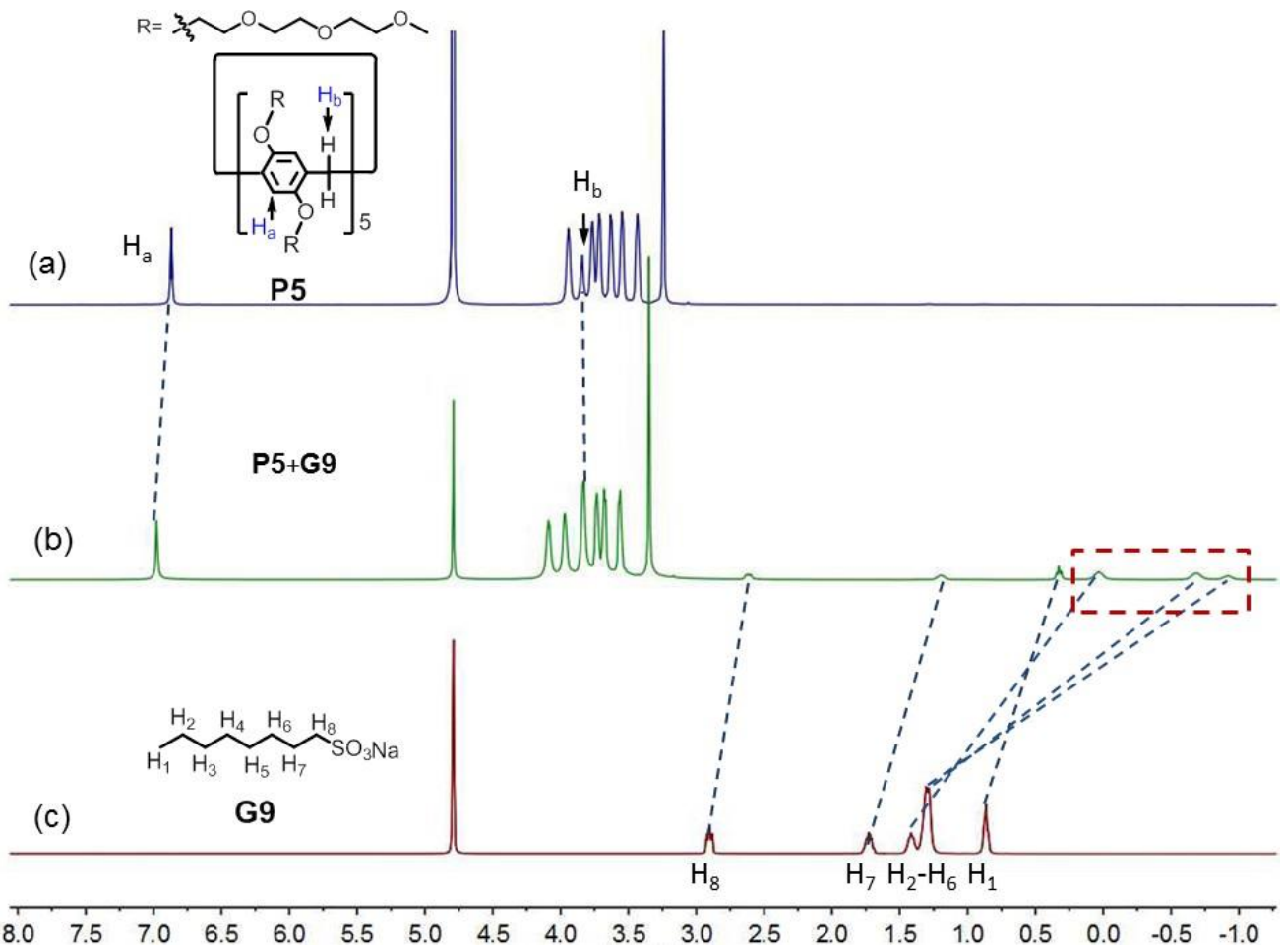

Figure S7. ^{1}H NMR spectra (400 MHz, D_2O, room temperature) of: (a) **P5** (2.00 mM); (b) **P5** (2.00 mM) and **G9** (2.00 mM); (c) **G9** (2.00 mM).

G9 is an organic salt with a long alkyl chain (with more than four CH_2 units). Guests with alkyl chains have the same binding mode with Pillar[5]arene, four consecutive CH_2 units will be located in the cavity of the pillar[5]arene *via* the multiple CH-π interactions.

From ^{1}H NMR spectra (Figure S6 and S7) and NOESY (Figure S50 and Figure S51) of **P5-G6** and **P5-G9**, after the complexation, up field NMR shifts are observed, indicating that these four CH_2 units are located in the cavity of **P5**, and the adjacent CH_2 units are near the rim of the cavity, and the driven forces are four CH-π interactions. However due the difference of groups in guest (imidazolium units in **G6** and SO_3^- in **G9**), the alkyl positions of **G6** and **G9** in P5 are different. Since no crystal structures are available, we cannot get the direct and detailed information about the location sites.

3. Stoichiometry and association constant determination for the complexation between **P5** and **G**

To determine the stoichiometry and association constant between **P5** and **G**, NMR titrations were done with solutions which had a constant concentration of **P5** (2 mM) and varying concentrations of **G**. G was dissolved in 2 mM P5 solution, so during the whole titration process, the concentration of **P5** is always 2 mM. With **P5⊃G1** as an example, by a non-linear curve-fitting method, the association constant (K_a) of **P5⊃G1** was estimated. By a mole ratio plot, a 1:1 stoichiometry was obtained.

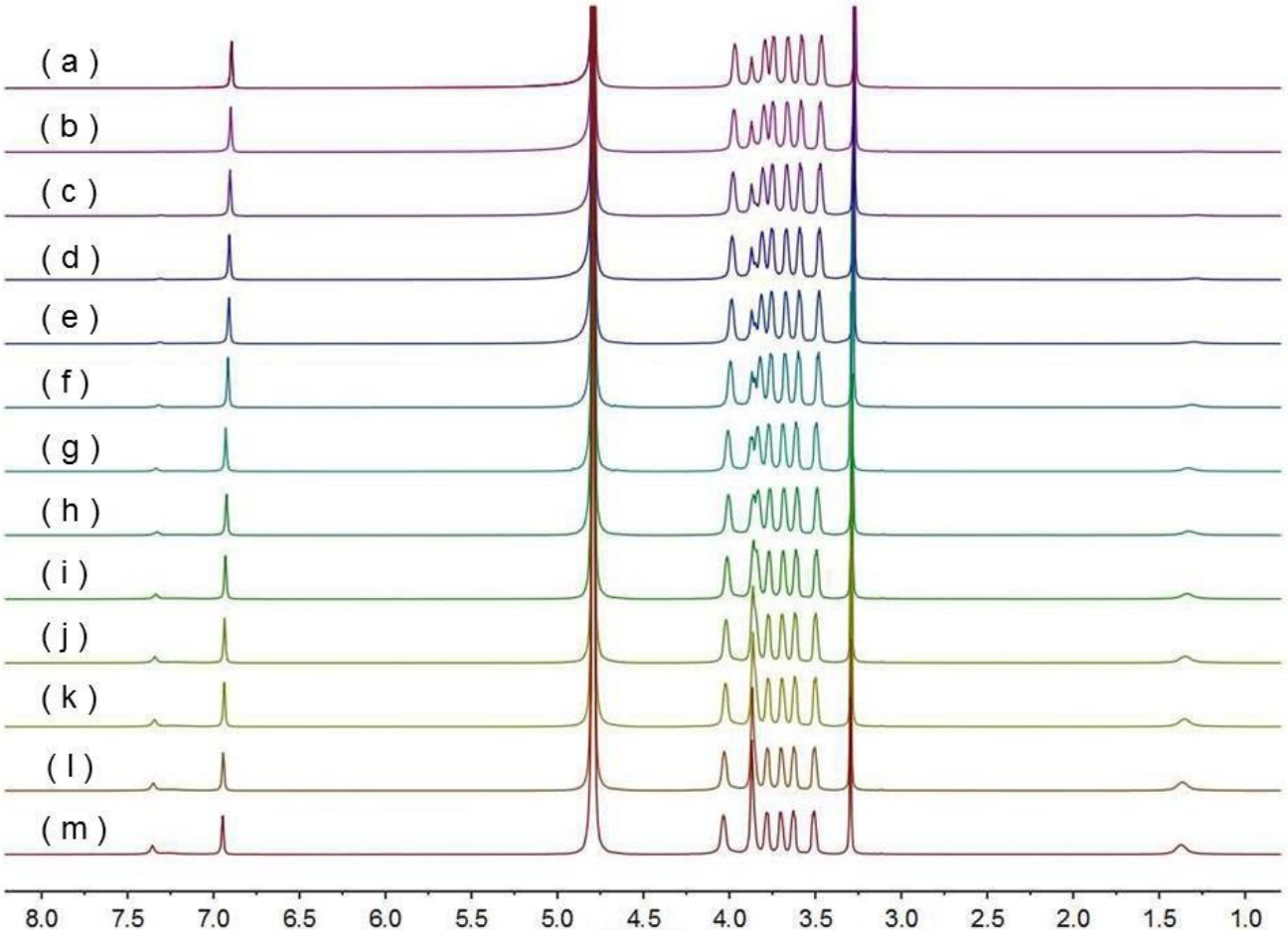

Figure S8. ^{1}H NMR spectra (400 MHz, D_2O, room temperature) of **P5** at a concentration of 2.0 mM upon addition of **G1** (15 mM): (a) 0.00 μL, (b) 10.00 μL, (c) 20.00 μL, (d) 30.00 μL, (e) 40.00 μL, (f) 65 μL, (g) 90.00 μL, (h) 115.00 μL, (i) 165.00 μL, (j) 215.00 μL, (k) 300.00 μL, (l) 360.00 μL, (m) 400.00 μL.

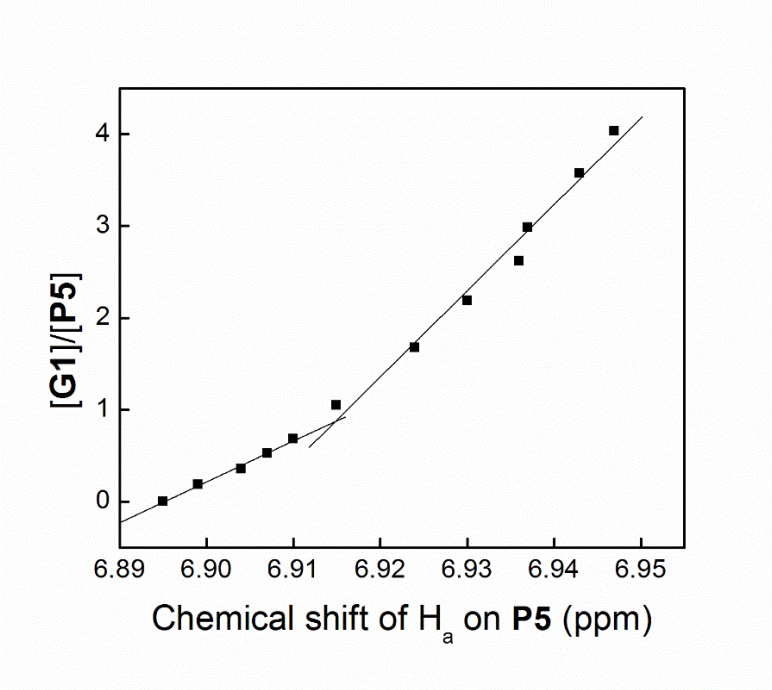

Figure S9. Mole ratio plot for **P5** and **G1**. The plot indicates a 1:1 stoichiometry.

The non-linear curve-fitting was based on the equation:[S2]

$\Delta\delta = (\Delta\delta_\infty/[H]_0)\ (0.5[G]_0 + 0.5([H]_0 + 1/Ka) - (0.5\ ([G]_0^2+(2[G]_0(1/Ka - [H]_0)) + (1/Ka + [H]_0)^2)^{0.5}))$ (Eq. S1)

Where $\Delta\delta$ is the chemical shift change of H_a on **P5** at $[G]_0$, $\Delta\delta_\infty$ is the chemical shift change of H_a when the host is completely complexed, $[H]_0$ is the fixed initial concentration of the host, and $[G]_0$ is the initial concentration of **G**.

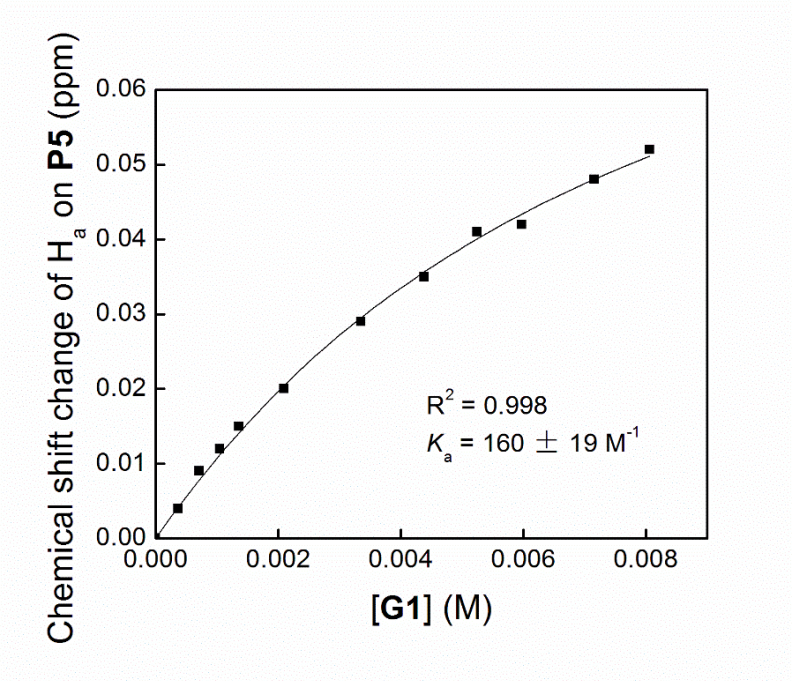

Figure S10. The chemical shift changes of H_a on **P5** upon addition of **G1**.

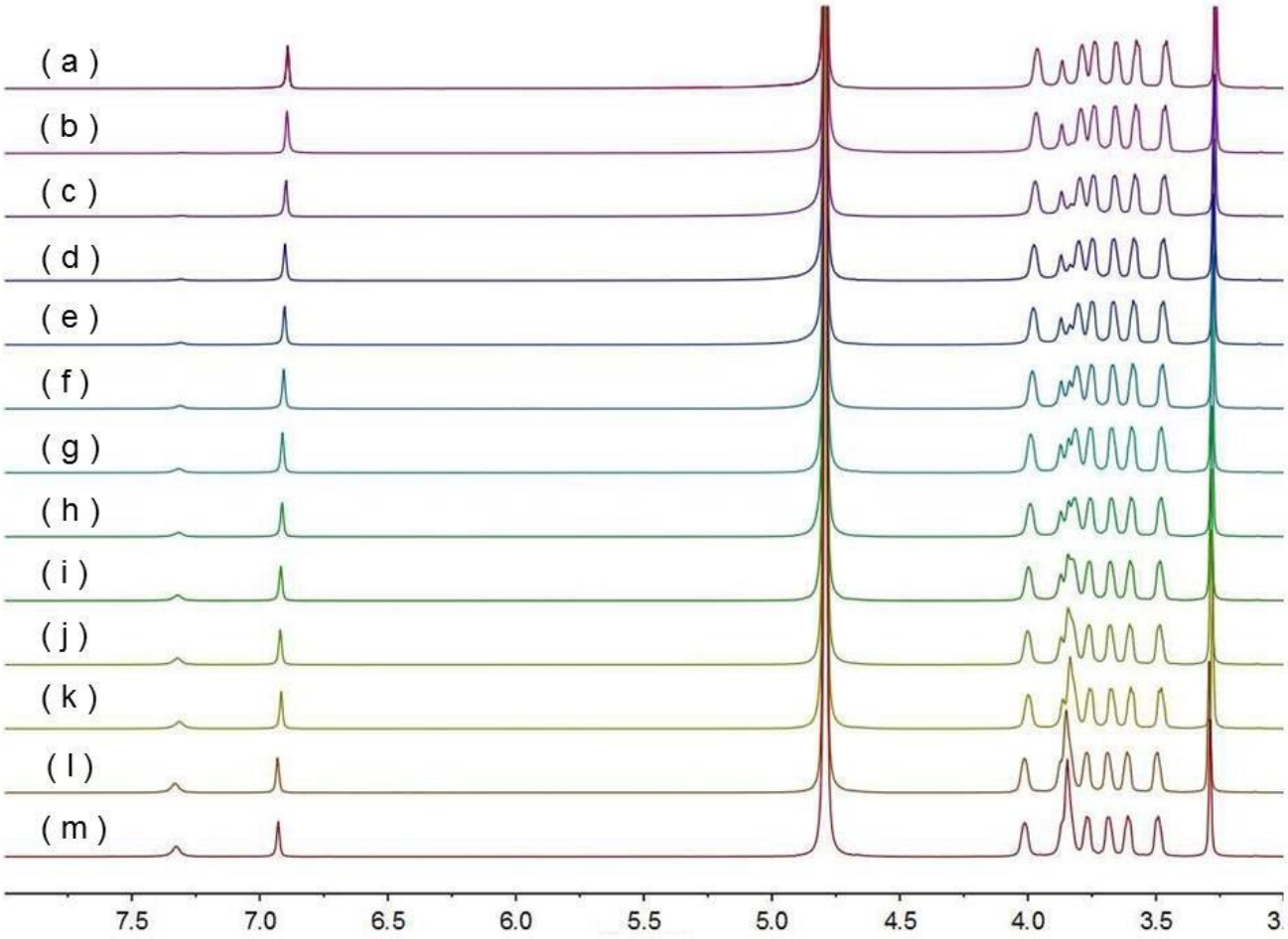

Figure S11. ^{1}H NMR spectra (400 MHz, D_2O, room temperature) of **P5** at a concentration of 2.0 mM upon addition of **G2** (15 mM): (a) 0.00 µL, (b) 10.00 µL, (c) 20.00 µL, (d) 30.00 µL, (e) 40.00 µL, (f) 65 µL, (g) 90.00 µL, (h) 115.00 µL, (i) 165.00 µL, (j) 215.00 µL, (k) 265.00 µL, (l) 365.00 µL, (m) 465.00µL

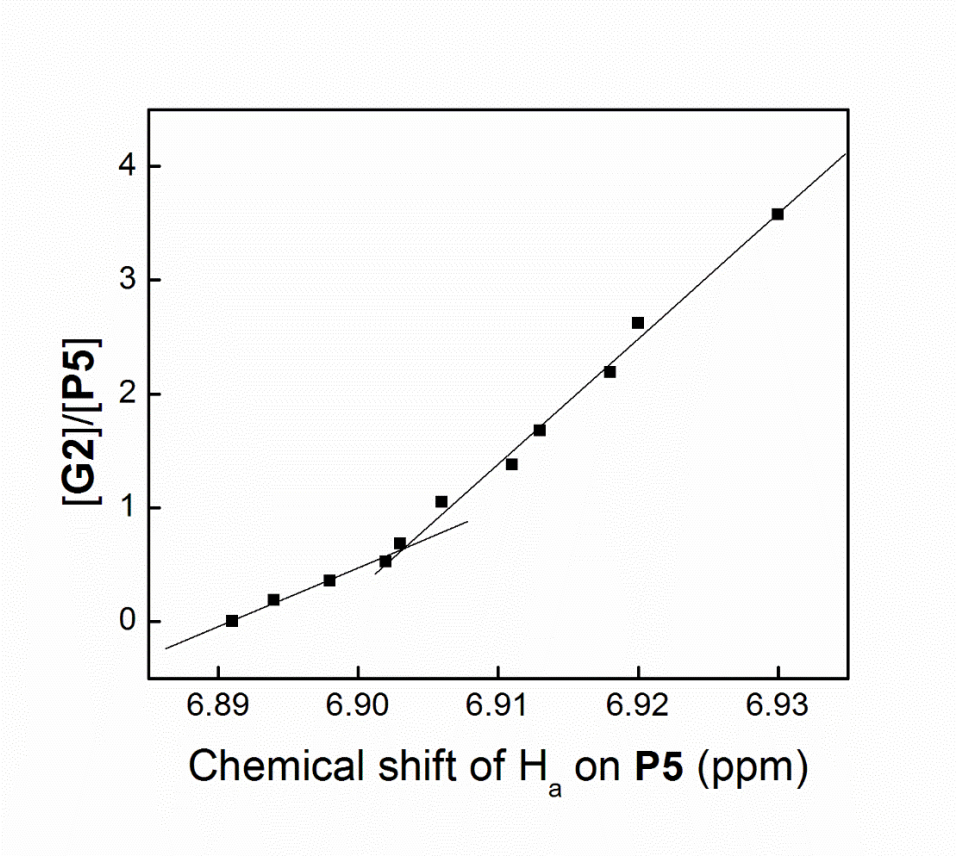

Figure S12. Mole ratio plot for **P5** and **G2**. The plot indicates a 1:1 stoichiometry.

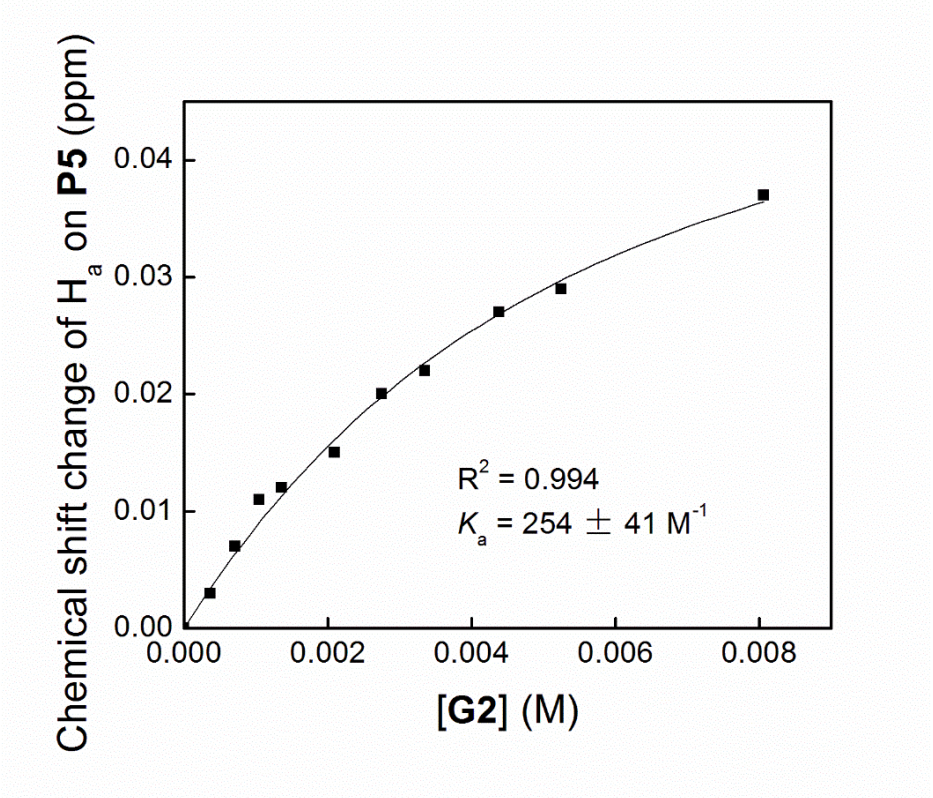

Figure S13. The chemical shift changes of H_a on **P5** upon addition of **G2**.

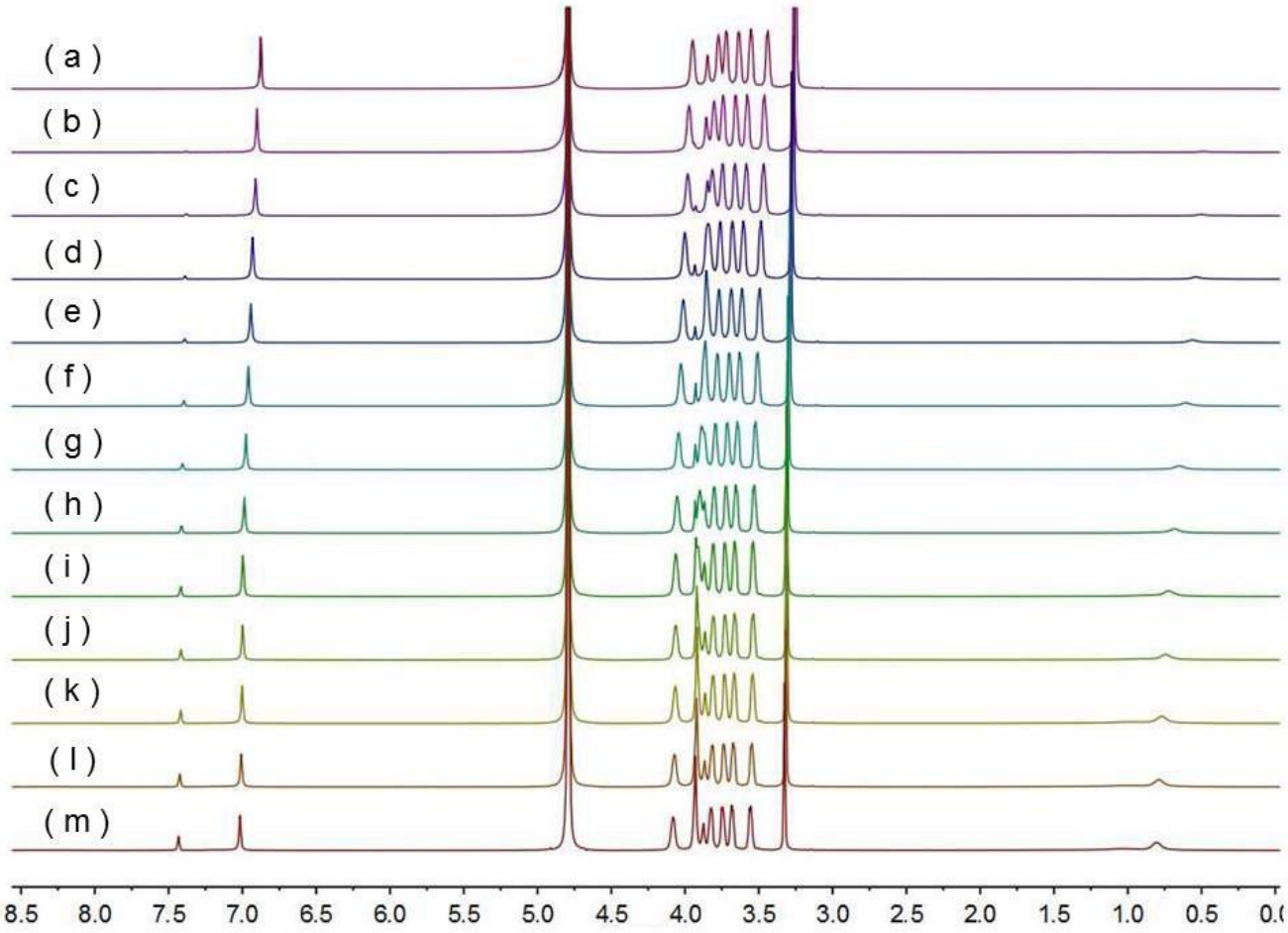

Figure S14. ^{1}H NMR spectra (400 MHz, D_2O, room temperature) of **P5** at a concentration of 2.0 mM upon addition of **G3** (15 mM): (a) 0.00 µL, (b) 10.00 µL, (c) 20.00 µL, (d) 30.00 µL, (e) 40.00 µL, (f) 65 µL, (g) 90.00 µL, (h) 115.00 µL, (i) 165.00 µL, (j) 215.00 µL, (k) 300.00 µL, (l) 360.00 µL, (m) 400.00 µL.

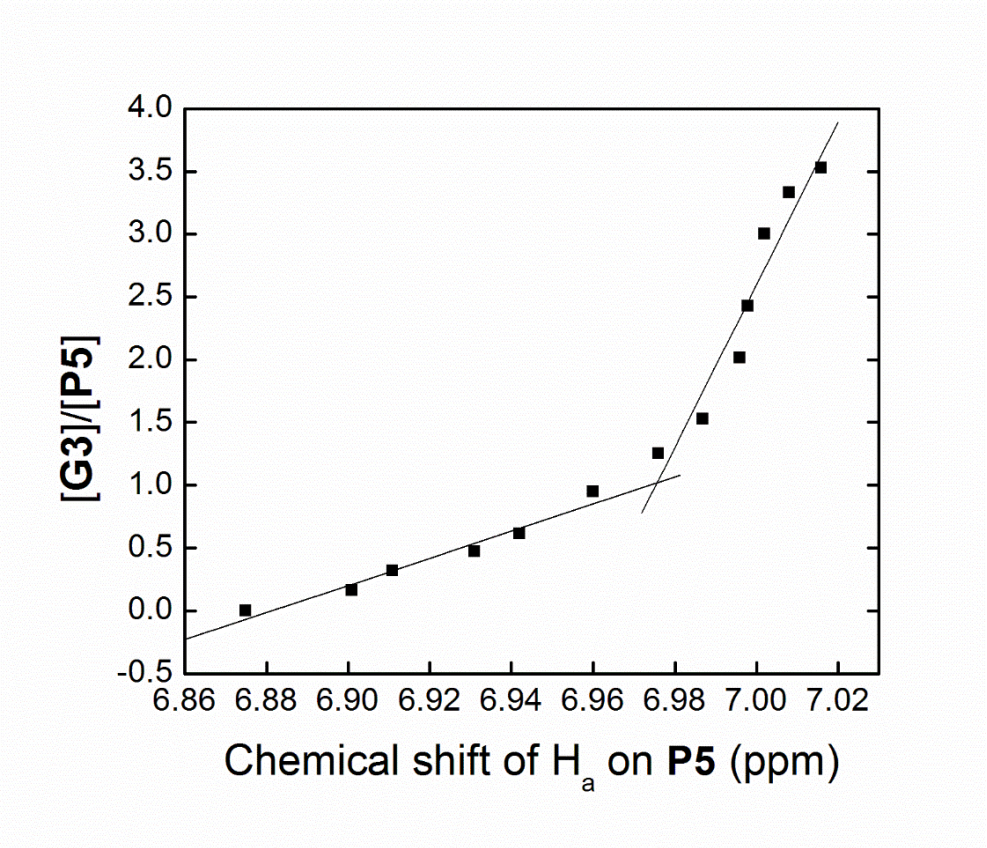

Figure S15. Mole ratio plot for **P5** and **G3**. The plot indicates a 1:1 stoichiometry.

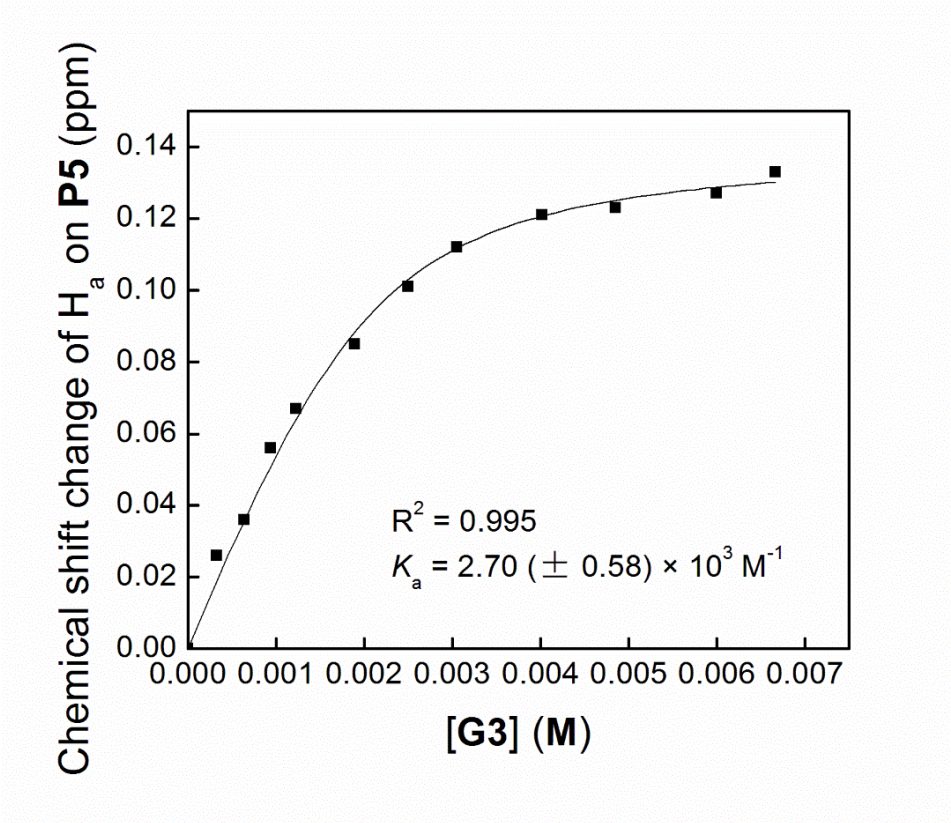

Figure S16. The chemical shift changes of H_a on **P5** upon addition of **G3**.

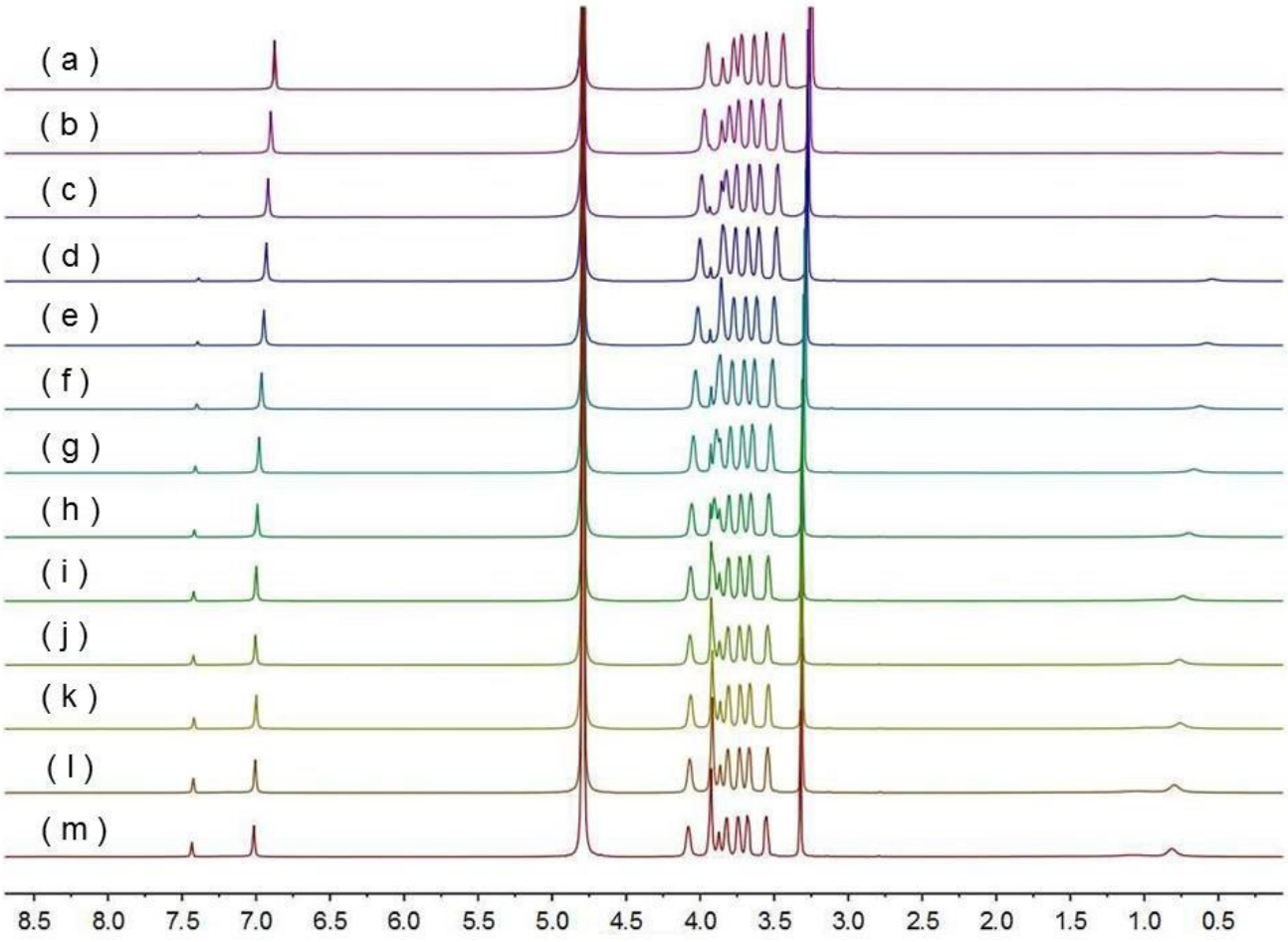

Figure S17. ^{1}H NMR spectra (400 MHz, D_2O, room temperature) of **P5** at a concentration of 2.0 mM upon addition of **G4** (15 mM): (a) 0.00 µL, (b) 10.00 µL, (c) 20.00 µL, (d) 30.00 µL, (e) 40.00 µL, (f) 65 µL, (g) 90.00 µL, (h) 115.00 µL, (i) 165.00 µL, (j) 215.00 µL, (k) 300.00 µL, (l) 360.00 µL, (m) 400.00 µL.

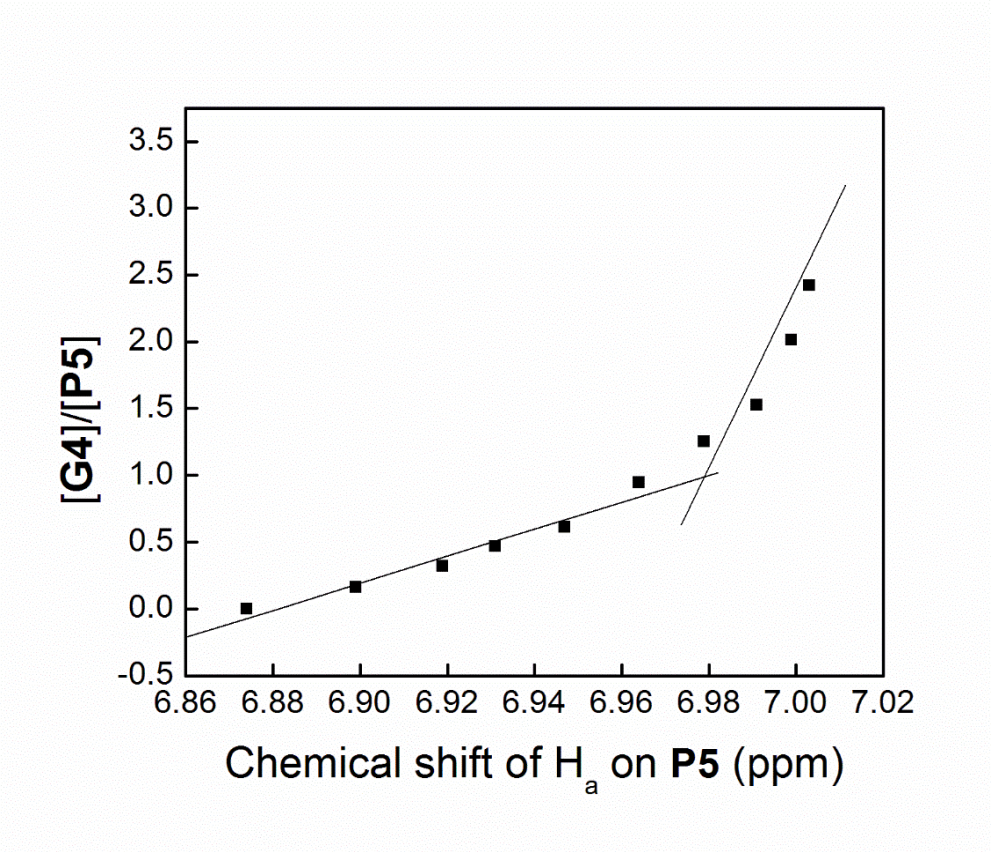

Figure S18. Mole ratio plot for **P5** and **G4**. The plot indicates a 1:1 stoichiometry.

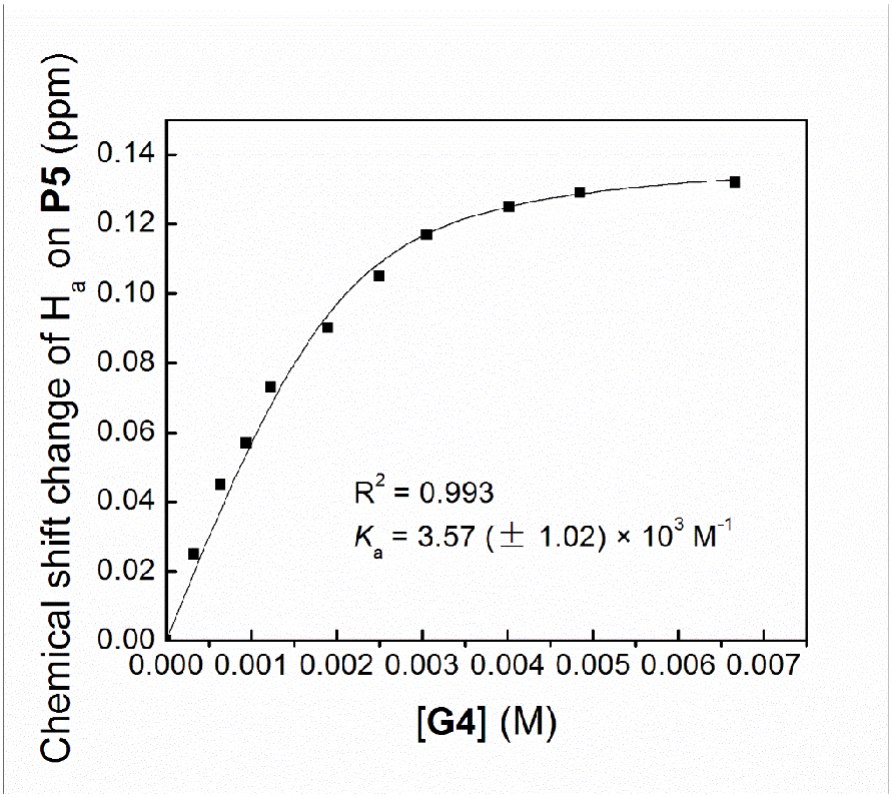

Figure S19. The chemical shift changes of H_a on **P5** upon addition of **G4**.

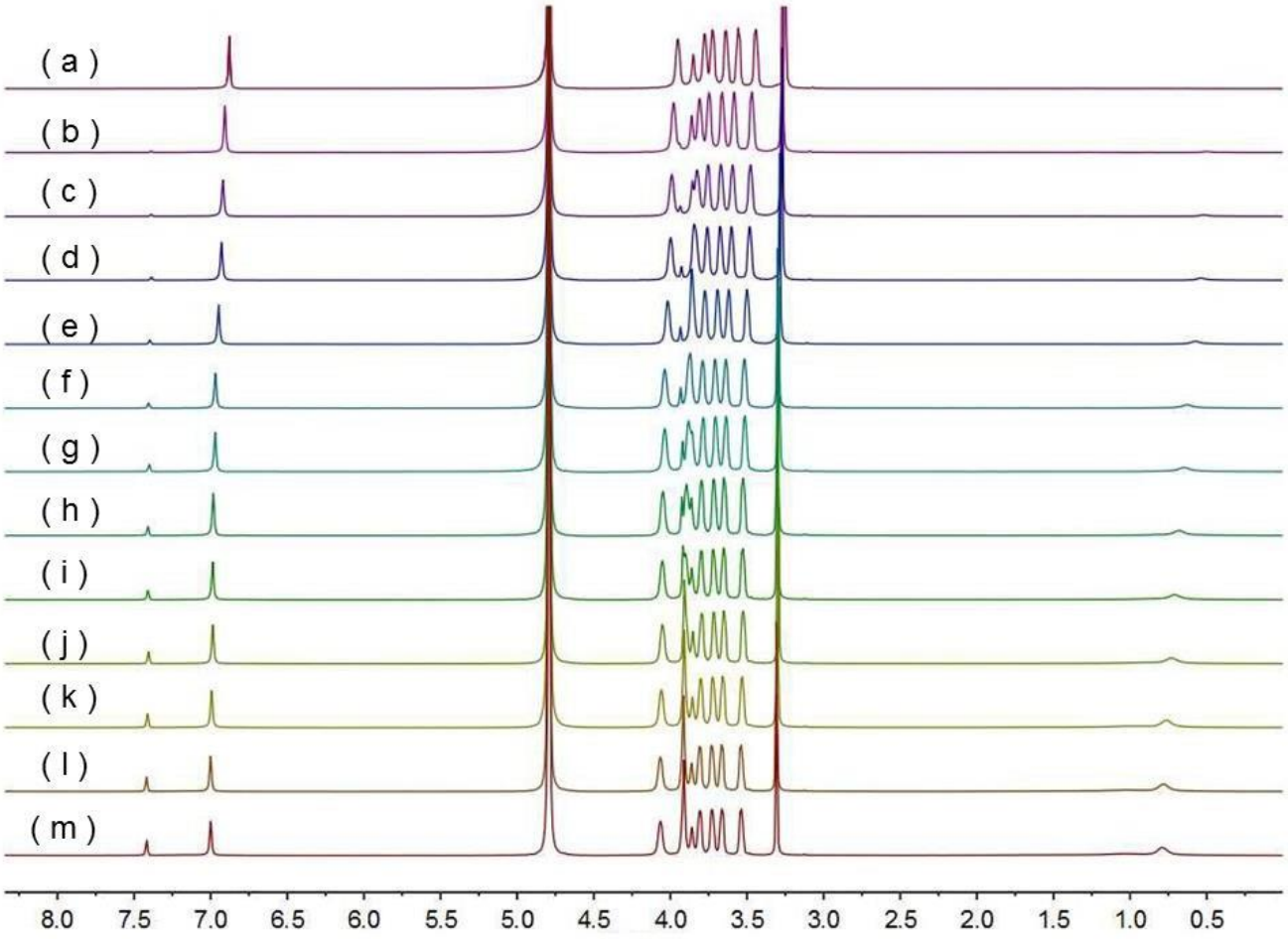

Figure S20. ^{1}H NMR spectra (400 MHz, D_2O, room temperature) of **P5** at a concentration of 2.0 mM upon addition of **G5** (15 mM): (a) 0.00 µL, (b) 10.00 µL, (c) 20.00 µL, (d) 30.00 µL, (e) 40.00 µL, (f) 65 µL, (g) 90.00 µL, (h) 115.00 µL, (i) 165.00 µL, (j) 215.00 µL, (k) 265.00 µL, (l) 365.00 µL, (m) 465.00 µL.

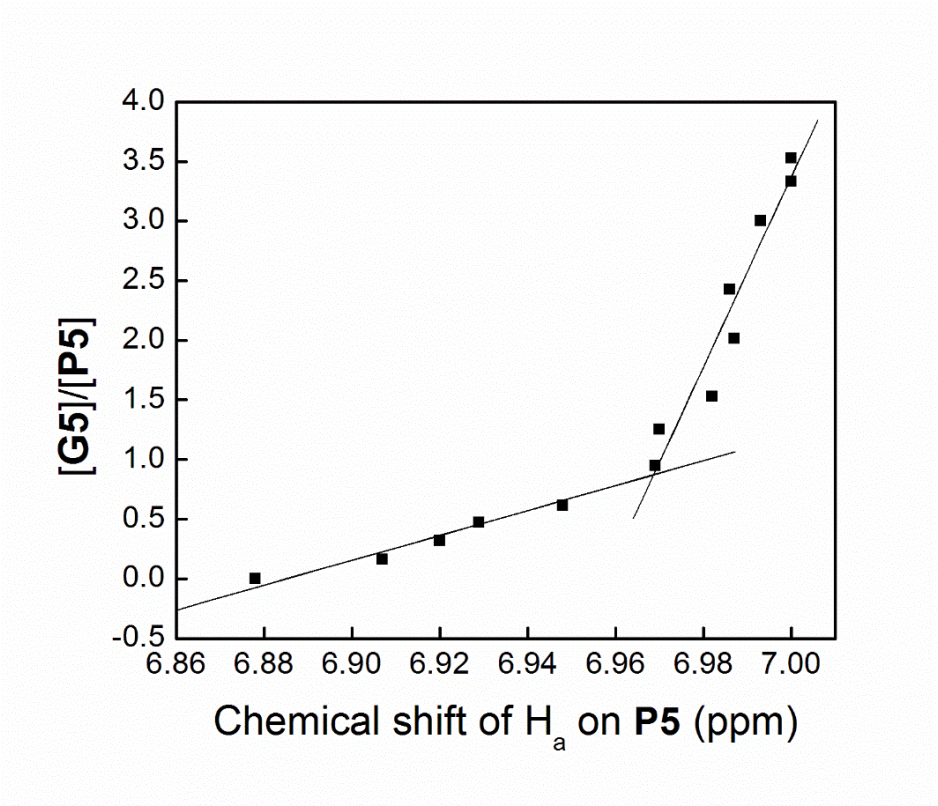

Figure S21. Mole ratio plot for **P5** and **G5**. The plot indicates a 1:1 stoichiometry.

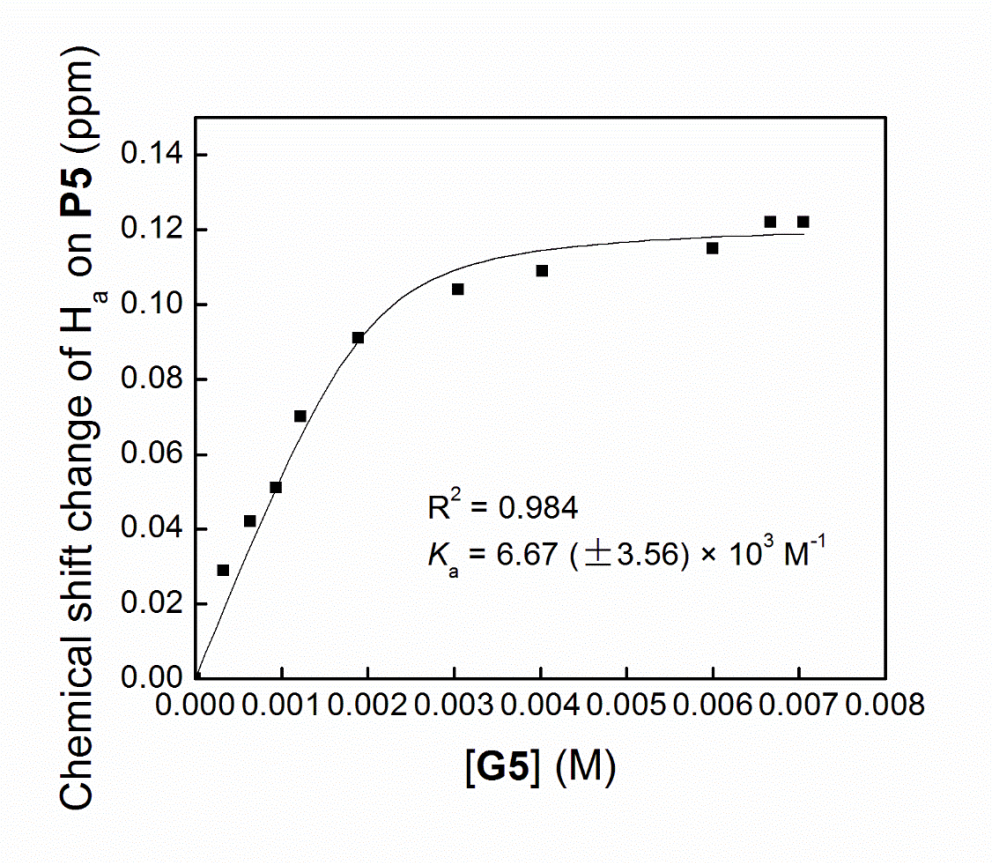

Figure S22. The chemical shift changes of H_a on **P5** upon addition of **G5**.

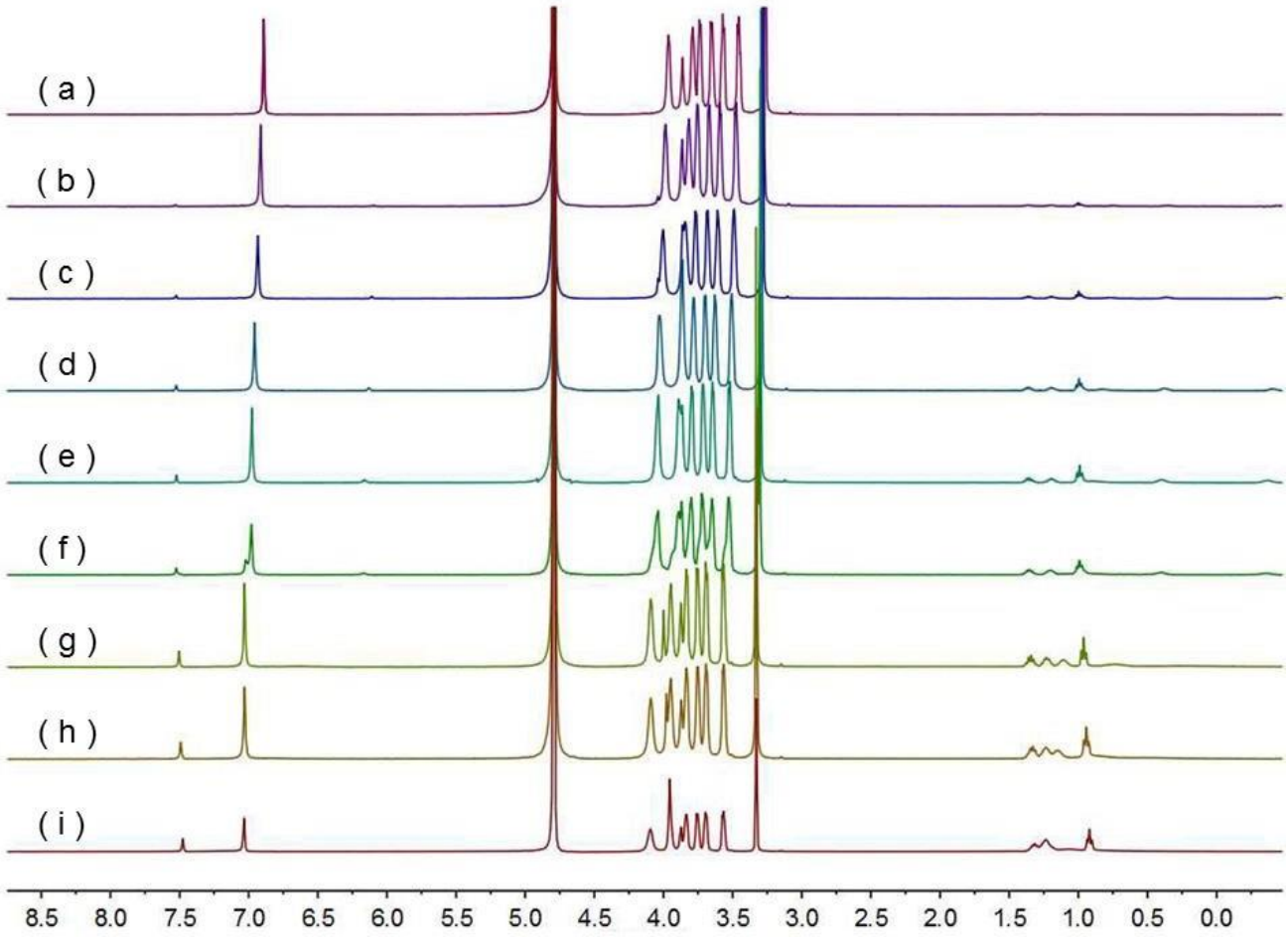

Figure S23. ^{1}H NMR spectra (400 MHz, D_2O, room temperature) of **P5** at a concentration of 2.0 mM upon addition of **G6** (15 mM): (a) 0.00 μL, (b) 10.00 μL, (c) 20.00 μL, (d) 30.00 μL, (e) 40.00 μL, (f) 65 μL, (g) 90.00 μL, (h) 115.00 μL, (i) 165.00 μL, (j) 215.00 μL, (k) 265.00 μL, (l) 365.00 μL, (m) 465.00 μL.

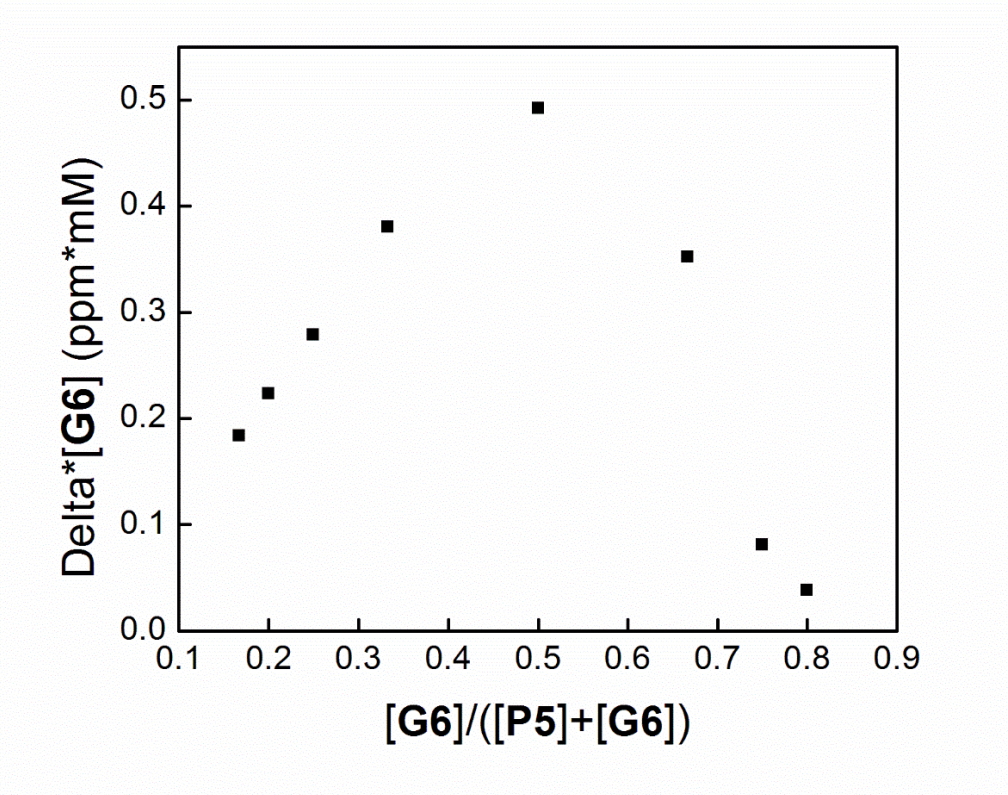

Figure S24. Job plot for **P5** and **G6**. job plot was conducted by varying the mole fractions of the guest and host. Concentration: [**P5**] + [**G6**] = 6 mM. The plot indicates a 1:1 binding between the host and guest.

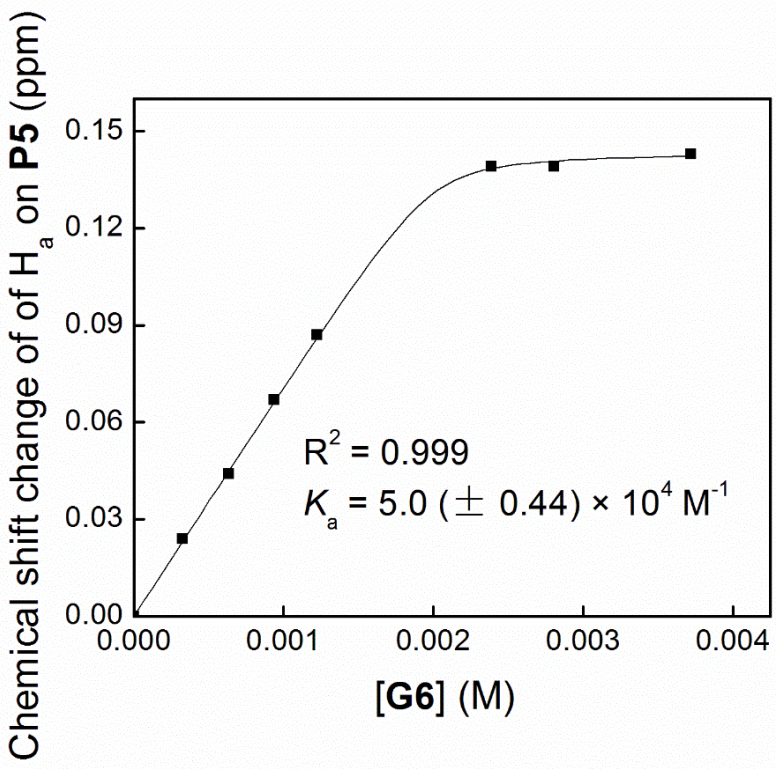

Figure S25. The chemical shift changes of H_a on **P5** upon addition of **G6**.

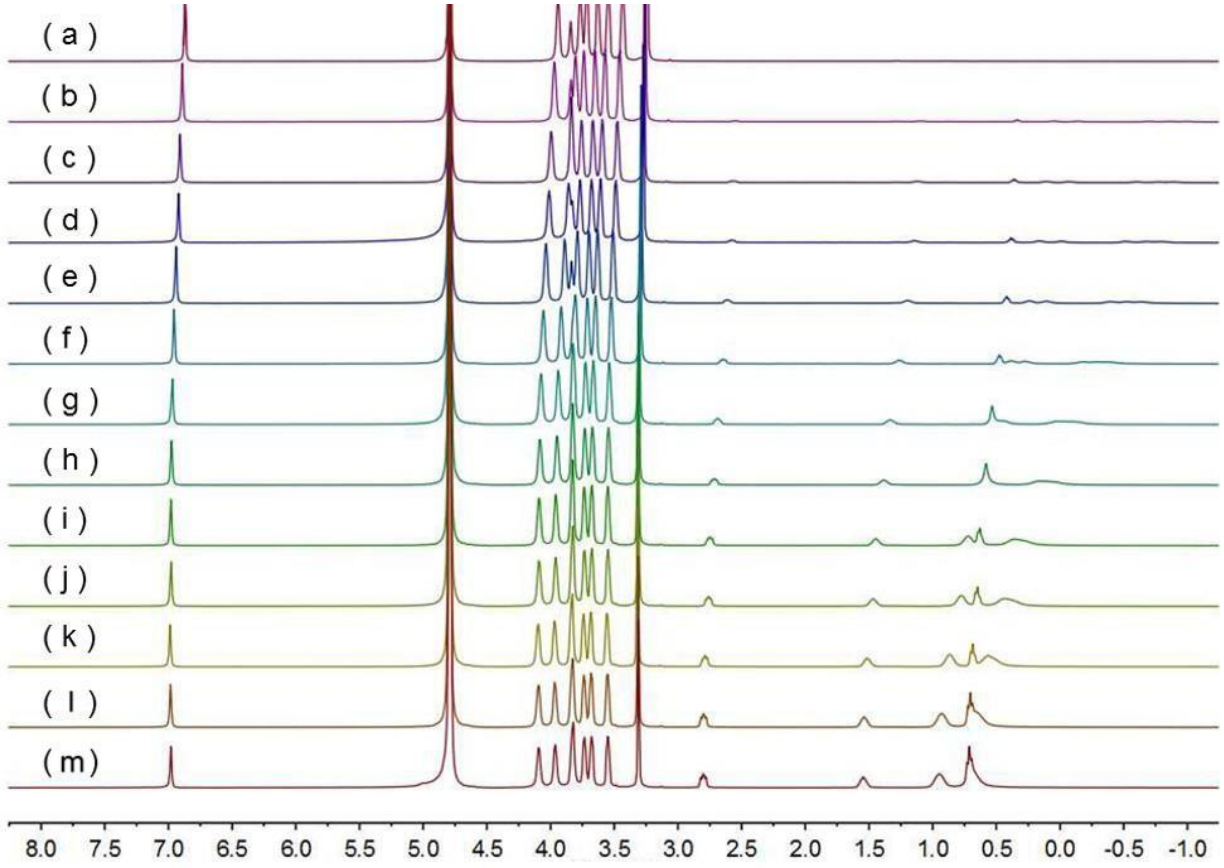

Figure S26. ^{1}H NMR spectra (400 MHz, D_2O, room temperature) of **P5** at a concentration of 2.0 mM upon addition of **G9** (15 mM): (a) 0.00 µL, (b) 10.00 µL, (c) 20.00 µL, (d) 30.00 µL, (e) 40.00 µL, (f) 65 µL, (g) 90.00 µL, (h) 115.00 µL, (i) 165.00 µL, (j) 215.00 µL, (k) 265.00 µL, (l) 365.00 µL, (m) 415.00 µL.

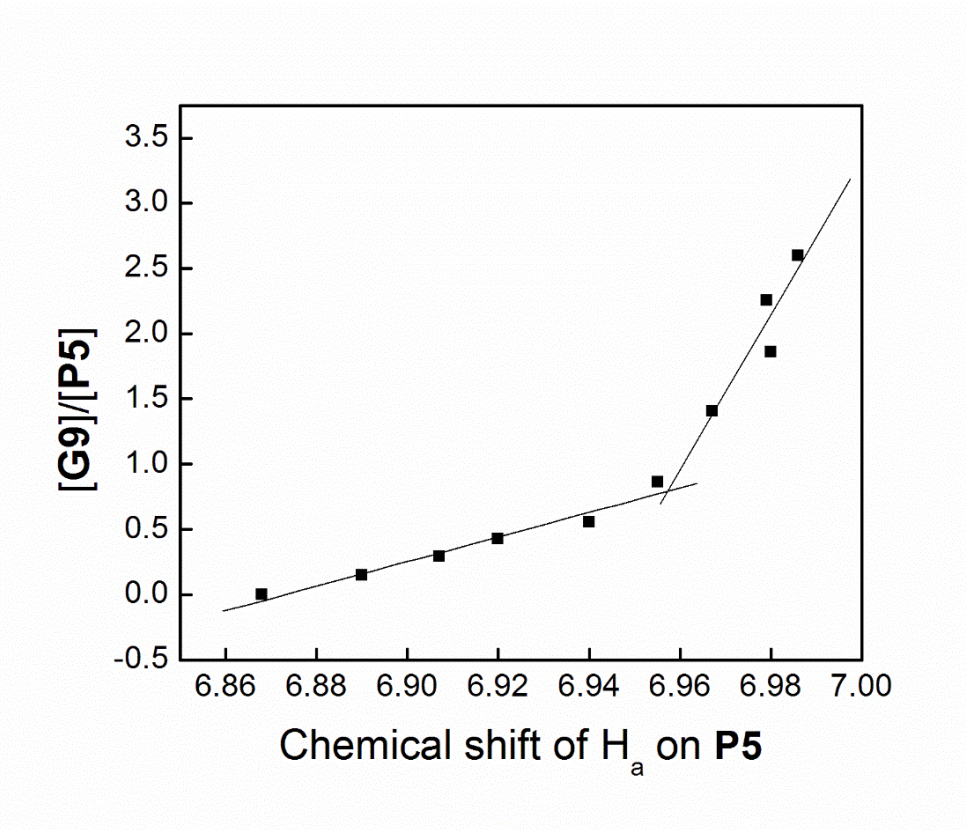

Figure S27. Mole ratio plot for **P5** and **G9**. The plot indicates a 1:1 binding between the host and guest.

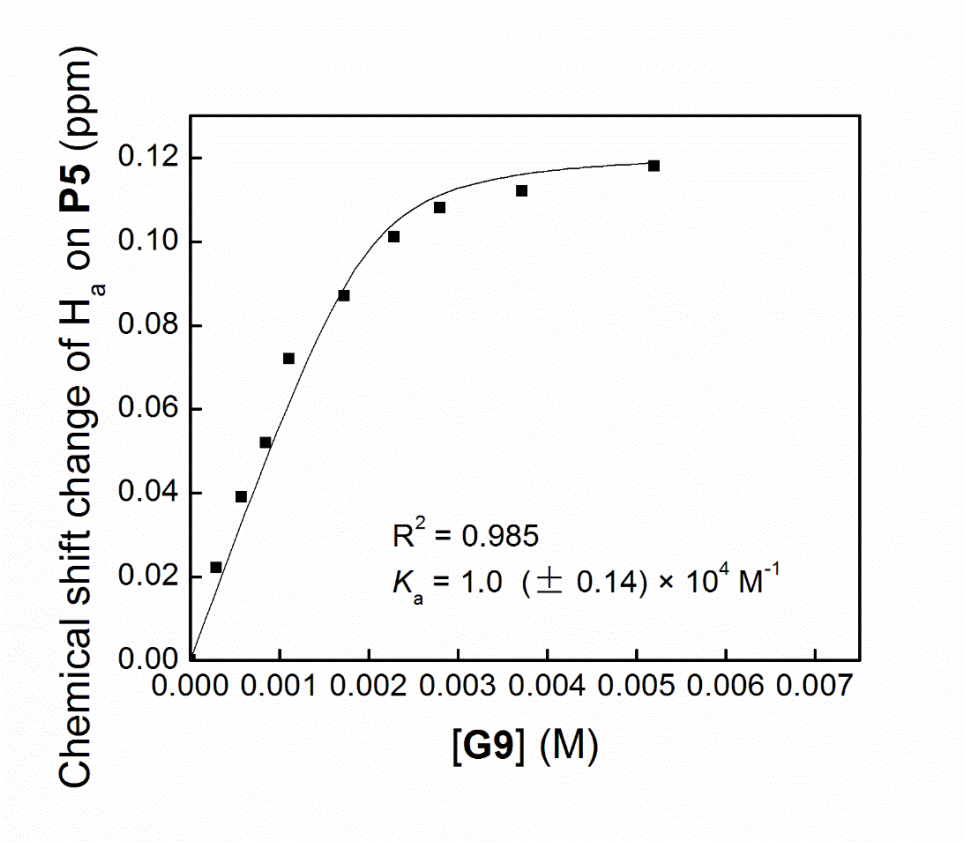

Figure S28. The chemical shift changes of H_a on **P5** upon addition of **G9**.

Guests	K_a (M^{-1})
G1	160 ± 19
G2	254 ± 3.56
G3	2.70 (± 0.58) × 10^3
G4	3.57 (± 1.02) × 10^3
G5	6.67 (± 3.56) × 10^3
G6	5.0 (± 0.44) × 10^4
G9	1.0 (± 0.14) × 10^4

Table S1. Association constant of host-guest complexes between **P5** and **G1-G6, G9**.

4. Mass spectra of host–guest complexes

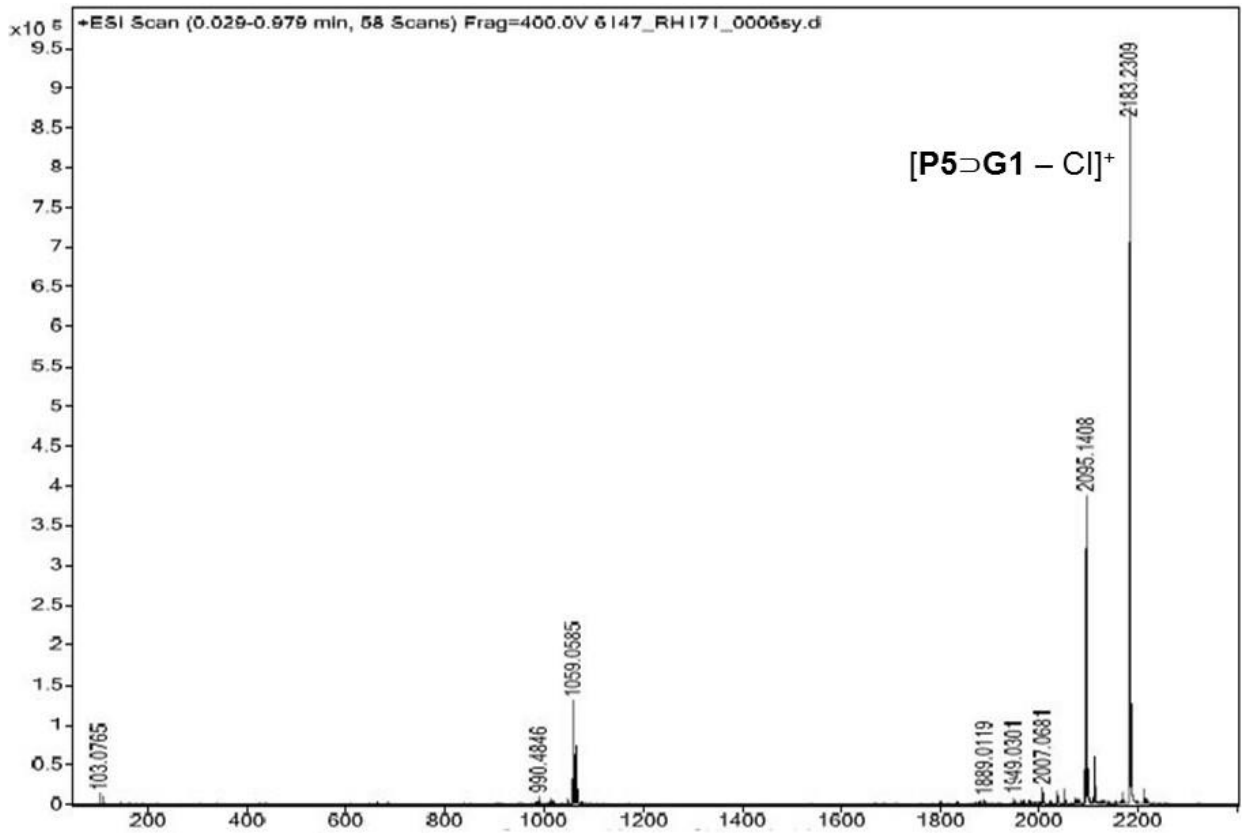

Figure S29. Mass spectrum of the host–guest complex prepared from **P5** and **G1**.

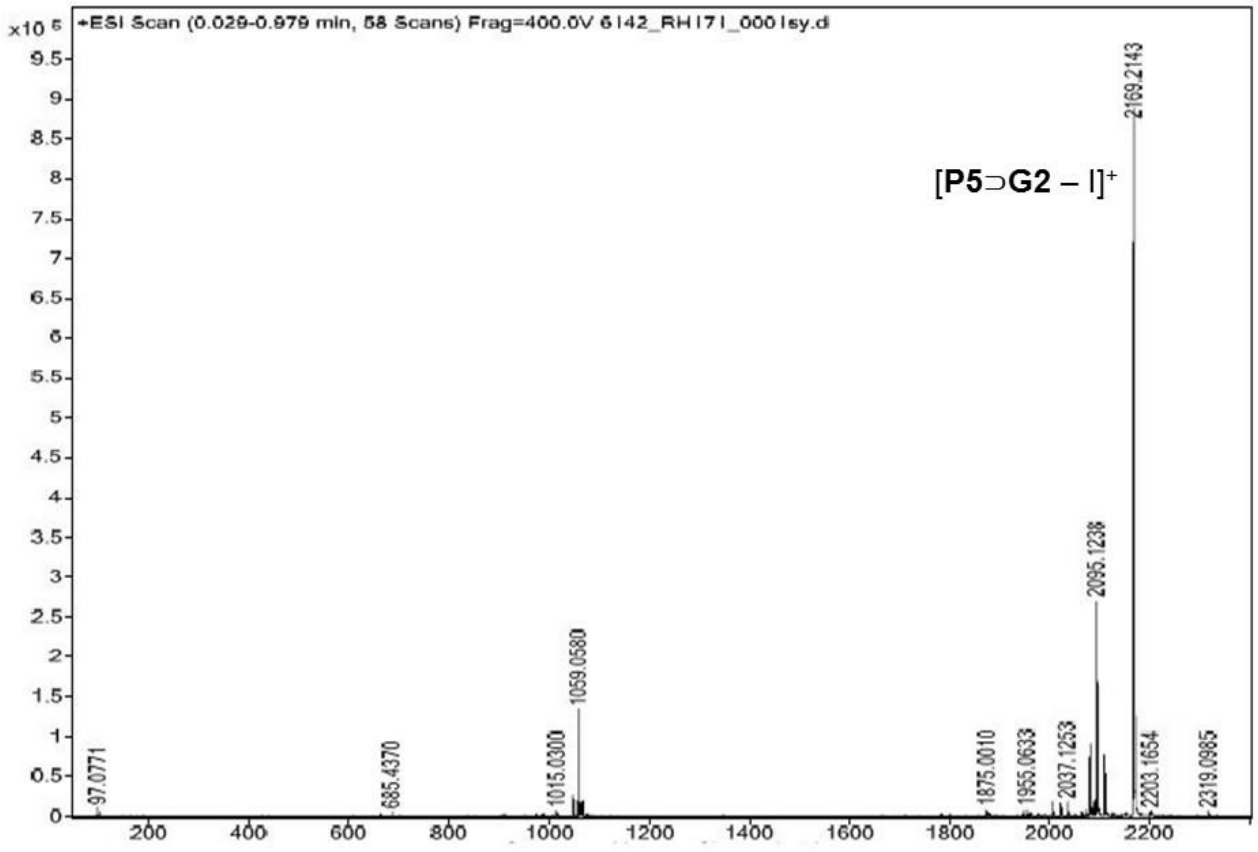

Figure S30. Mass spectrum of the host–guest complex prepared from **P5** and **G2**.

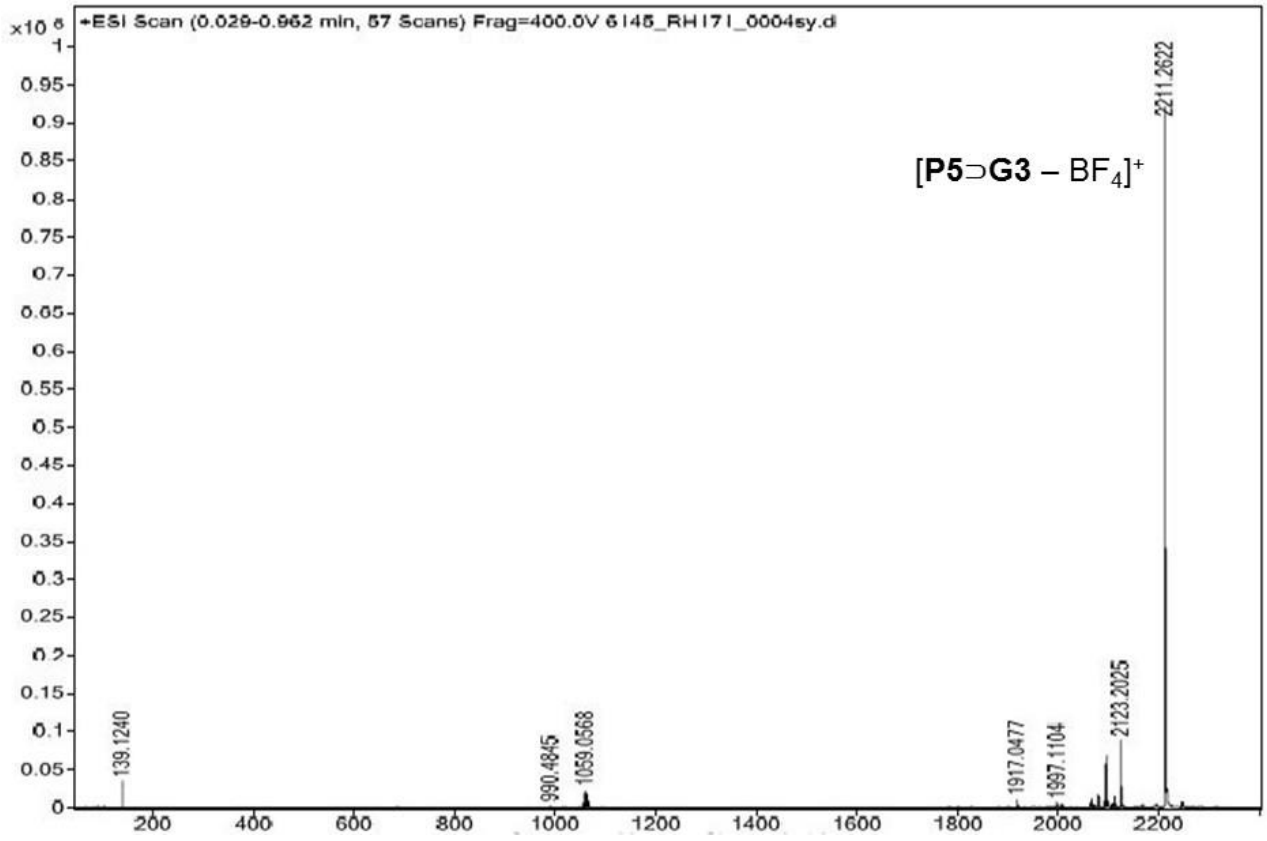

Figure S31. Mass spectrum of the host–guest complex prepared from **P5** and **G3**.

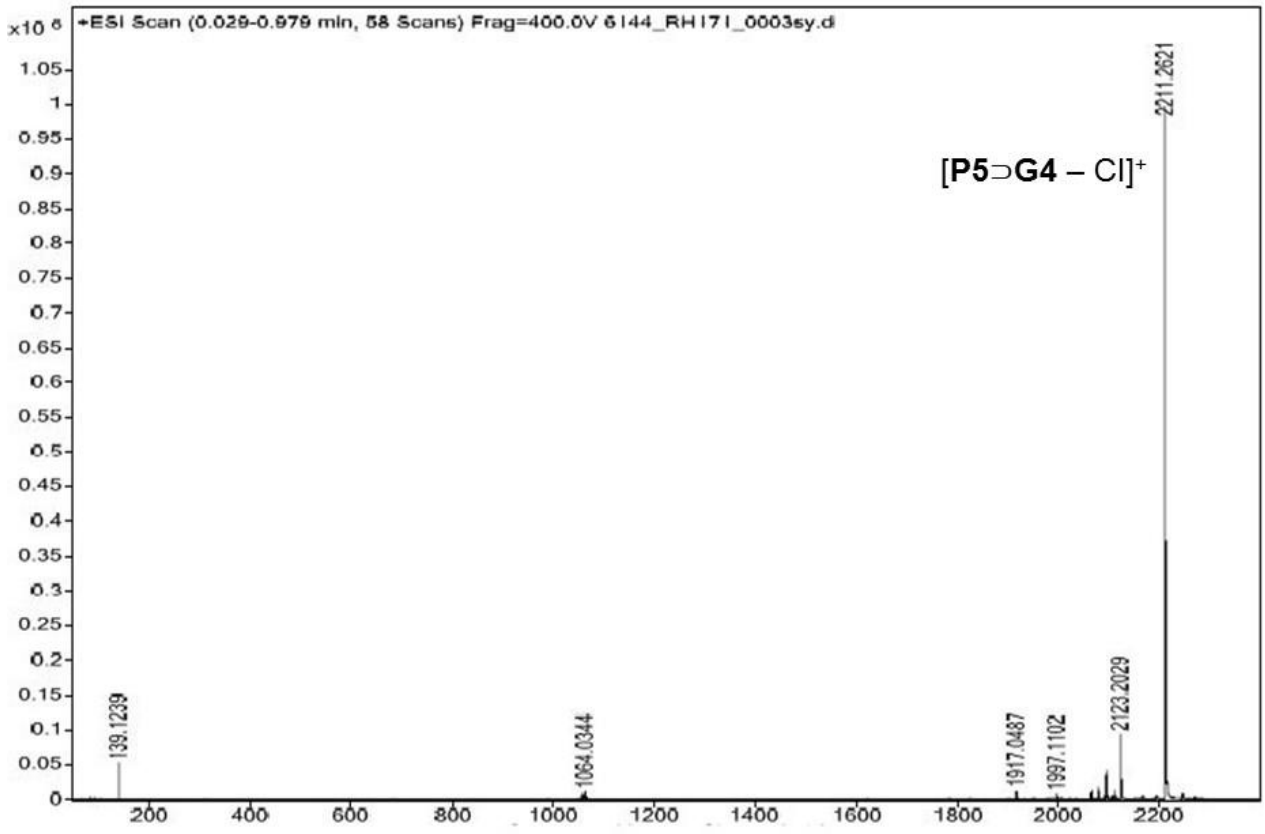

Figure S32. Mass spectrum of the host–guest complex prepared from **P5** and **G4**.

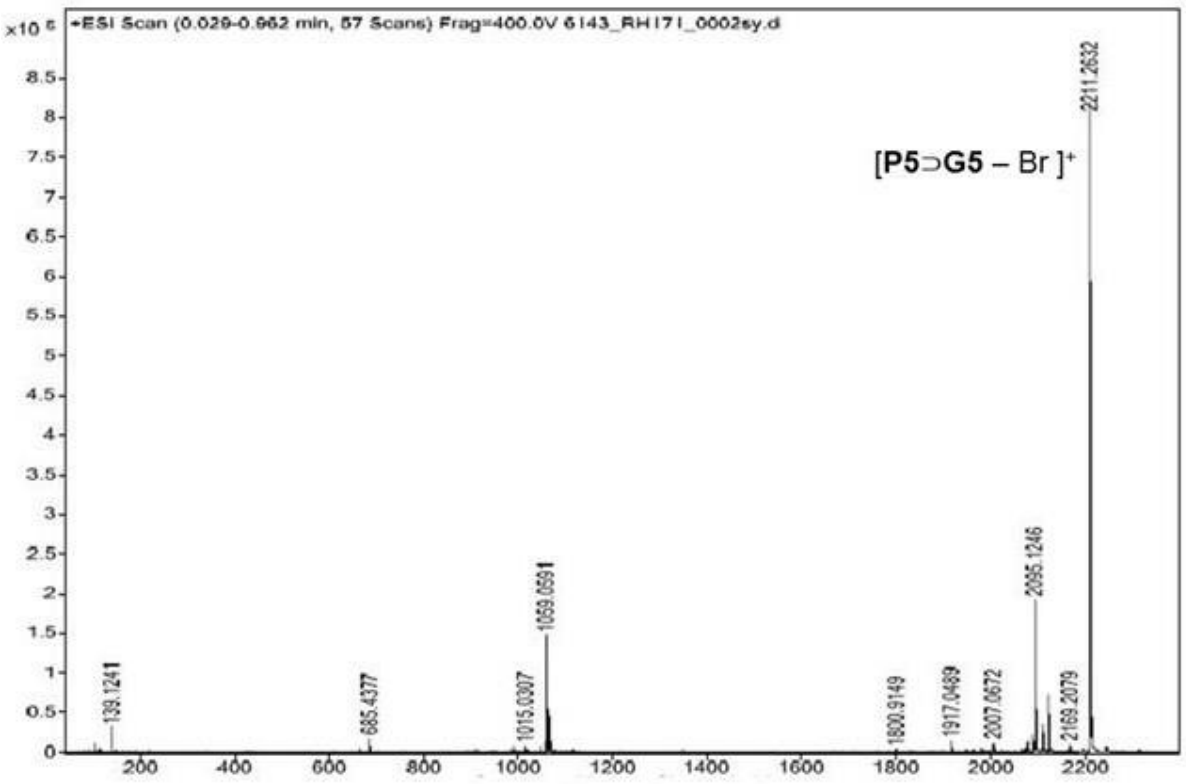

Figure S33. Mass spectrum of the host–guest complex prepared from **P5** and **G5**.

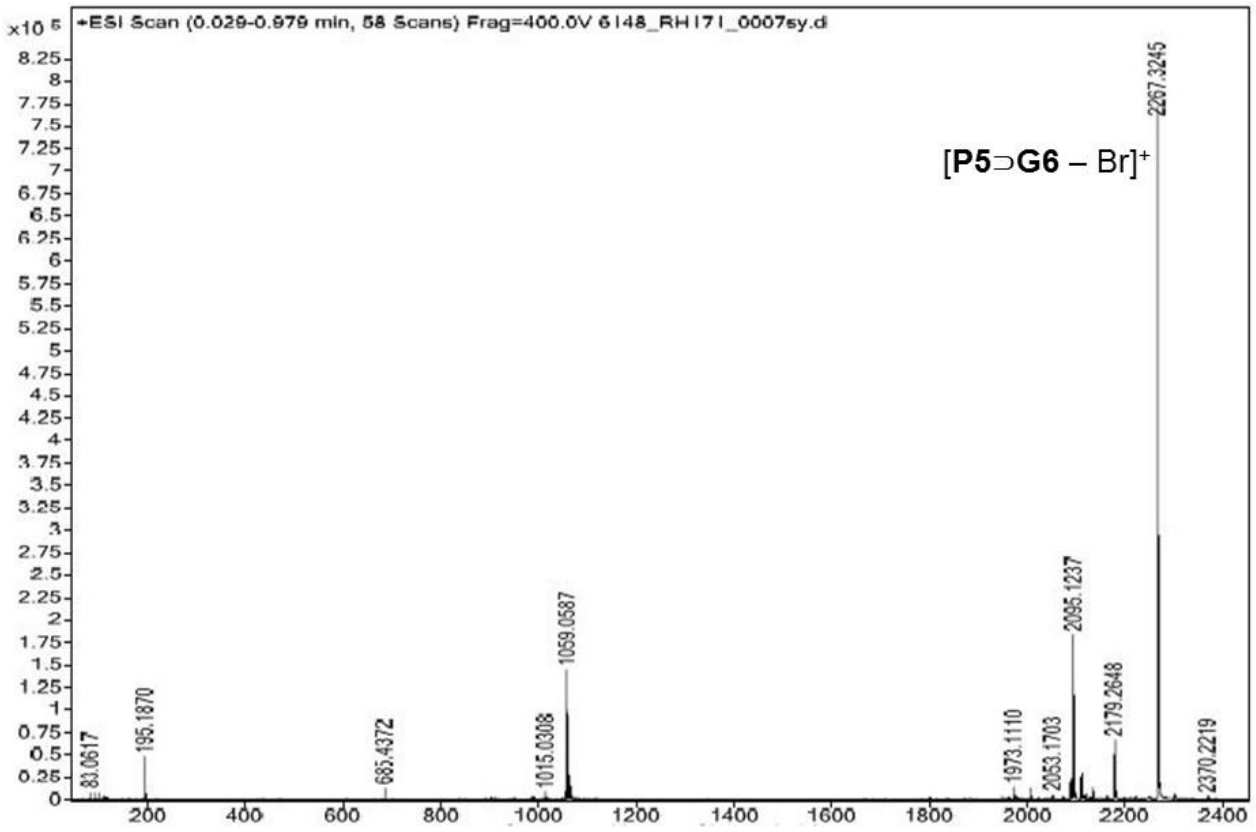

Figure S34. Mass spectrum of the host–guest complex prepared from **P5** and **G6**.

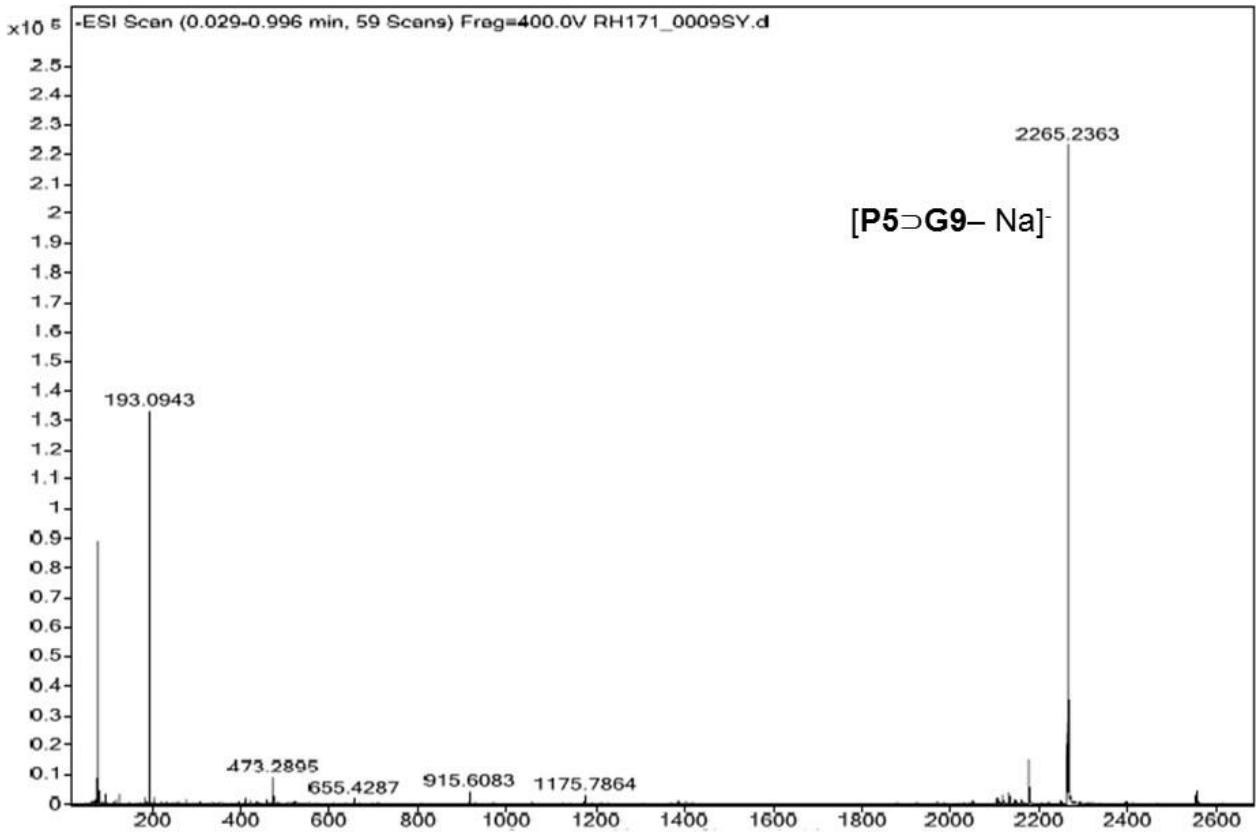

Figure S35. Mass spectrum of the host–guest complex prepared from **P5** and **G9**.

5. Temperature dependence NMR spectra of **P5** upon addition of guests

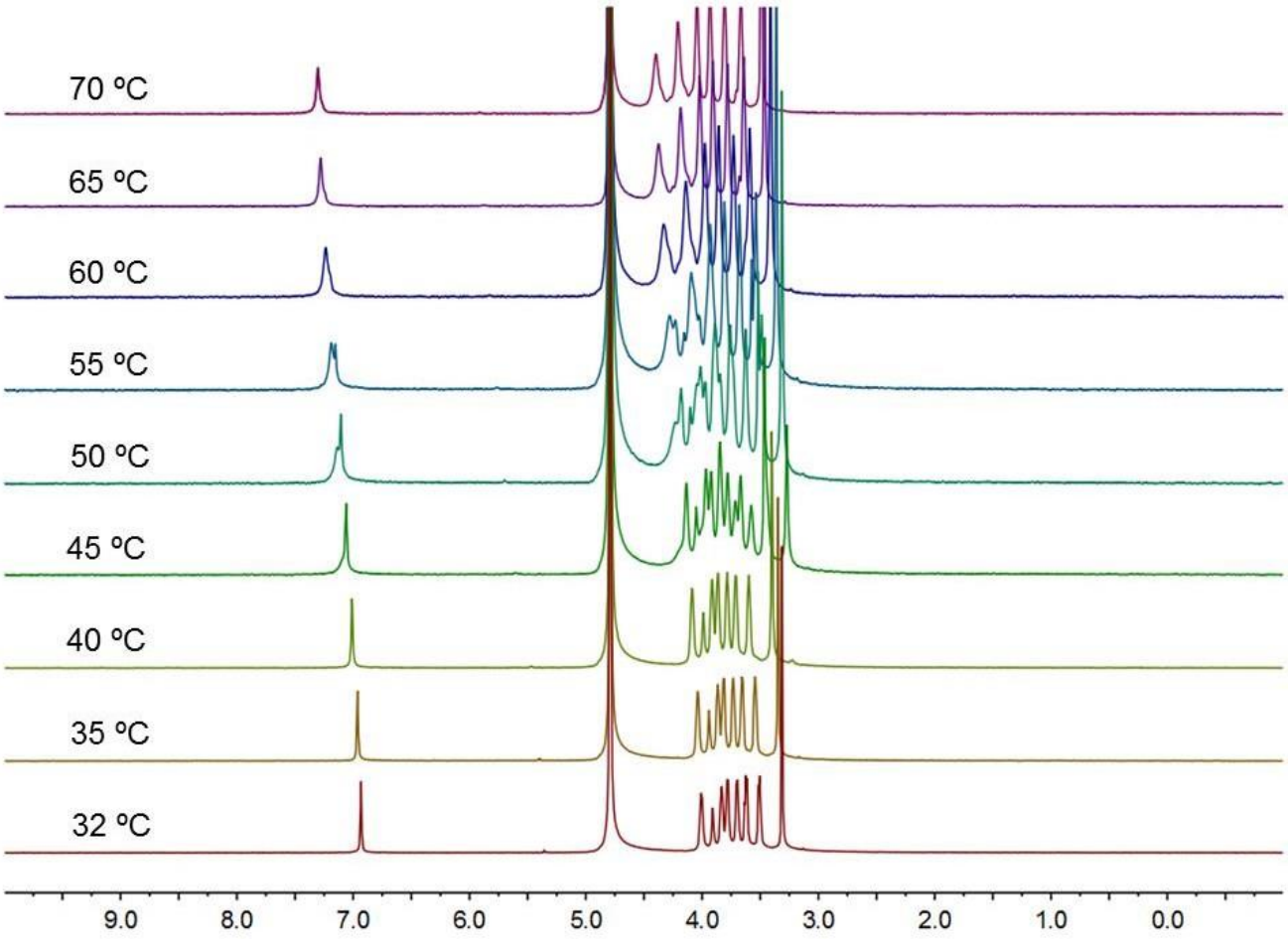

Figure S36. Variable-temperature ^{1}H NMR spectra (400 MHz) of **P5** (2.00 mM) in D_2O.

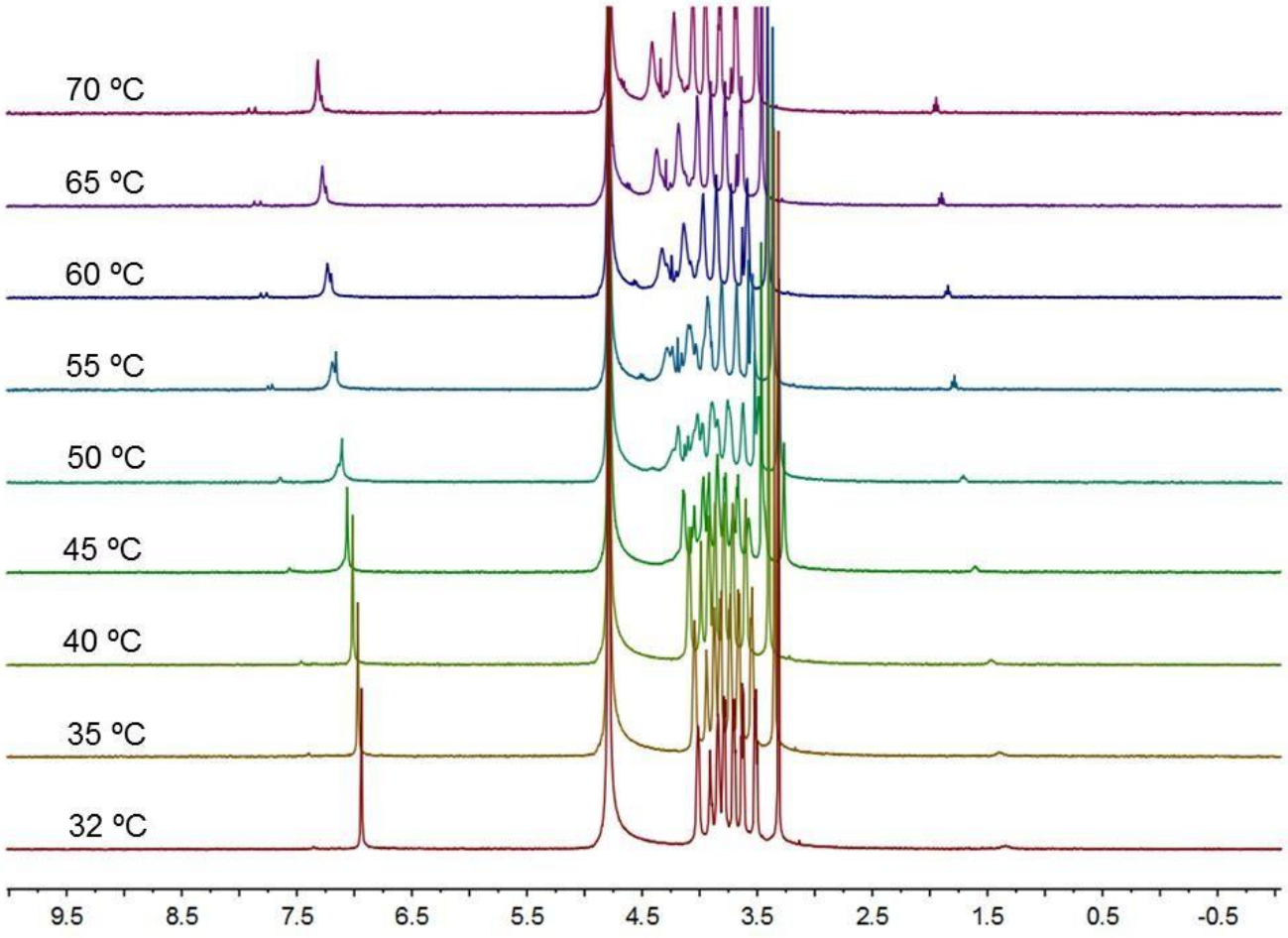

Figure S37. Variable-temperature ^{1}H NMR spectra (400 MHz) of **P5** and **G1** (2.00 mM) in D_2O.

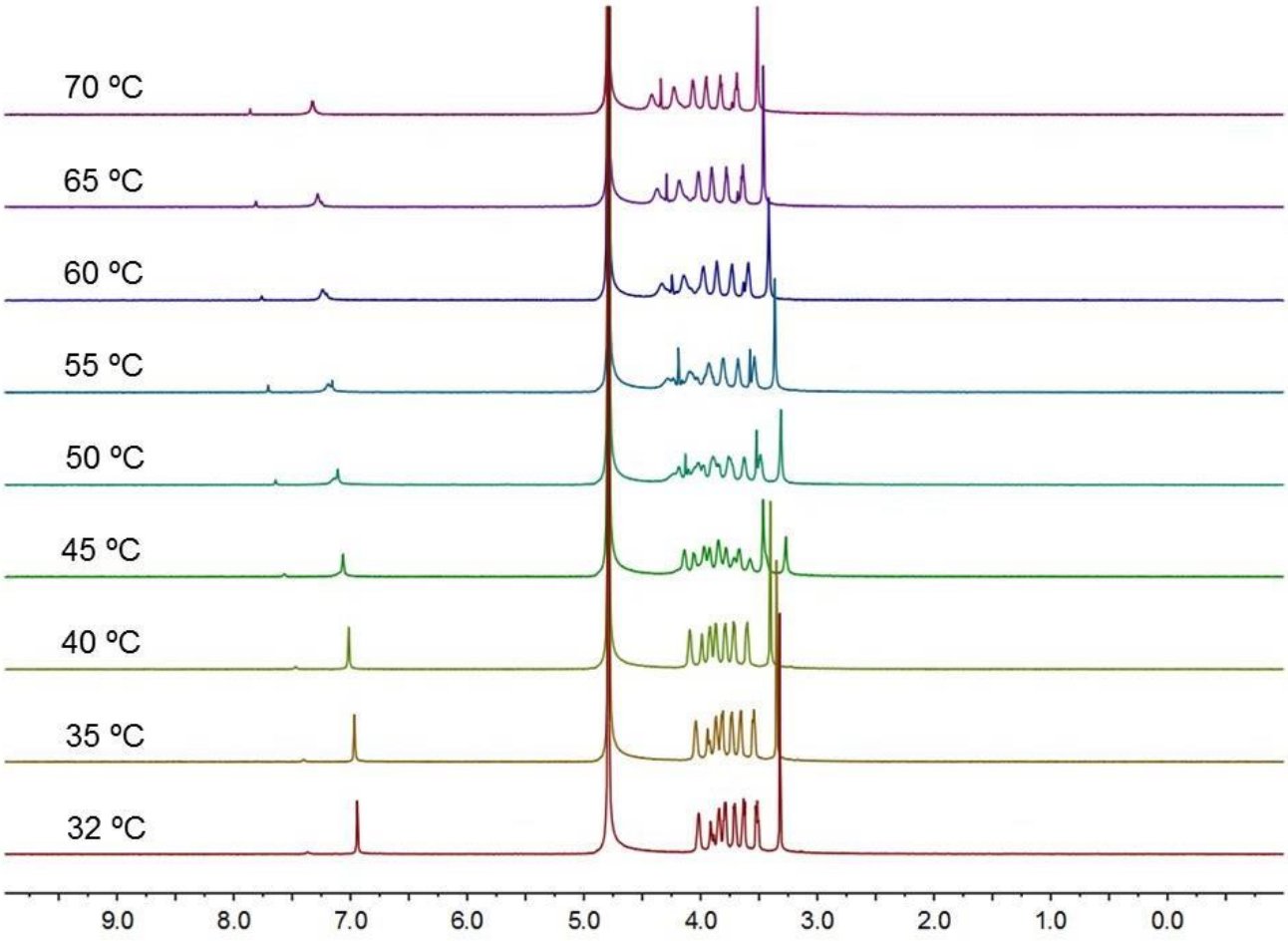

Figure S38. Variable-temperature ^{1}H NMR spectra (400 MHz) of **P5** and **G2** (2.00 mM) in D_2O.

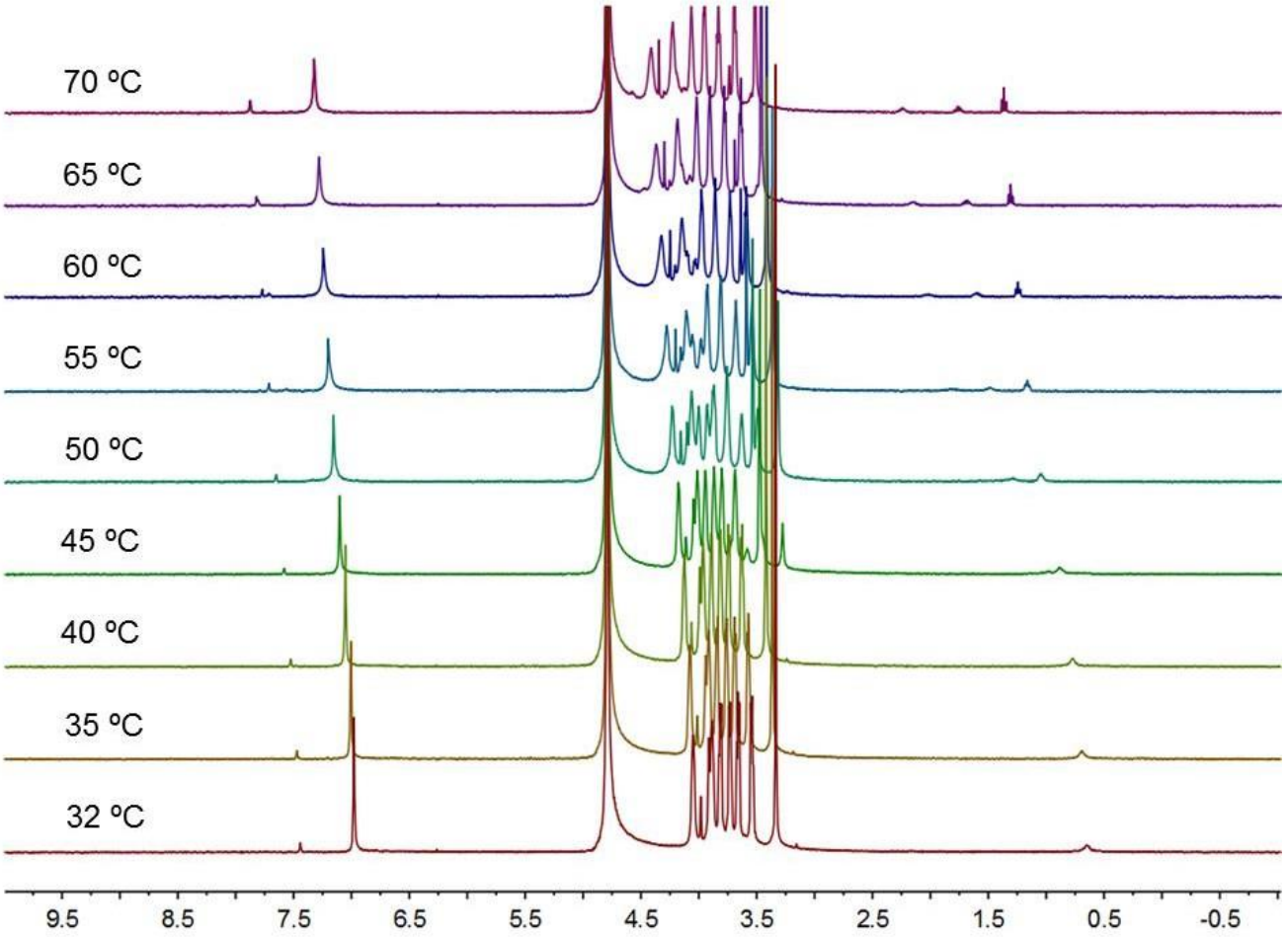

Figure S39. Variable-temperature ^{1}H NMR spectra (400 MHz) of **P5** and **G3** (2.00 mM) in D_2O.

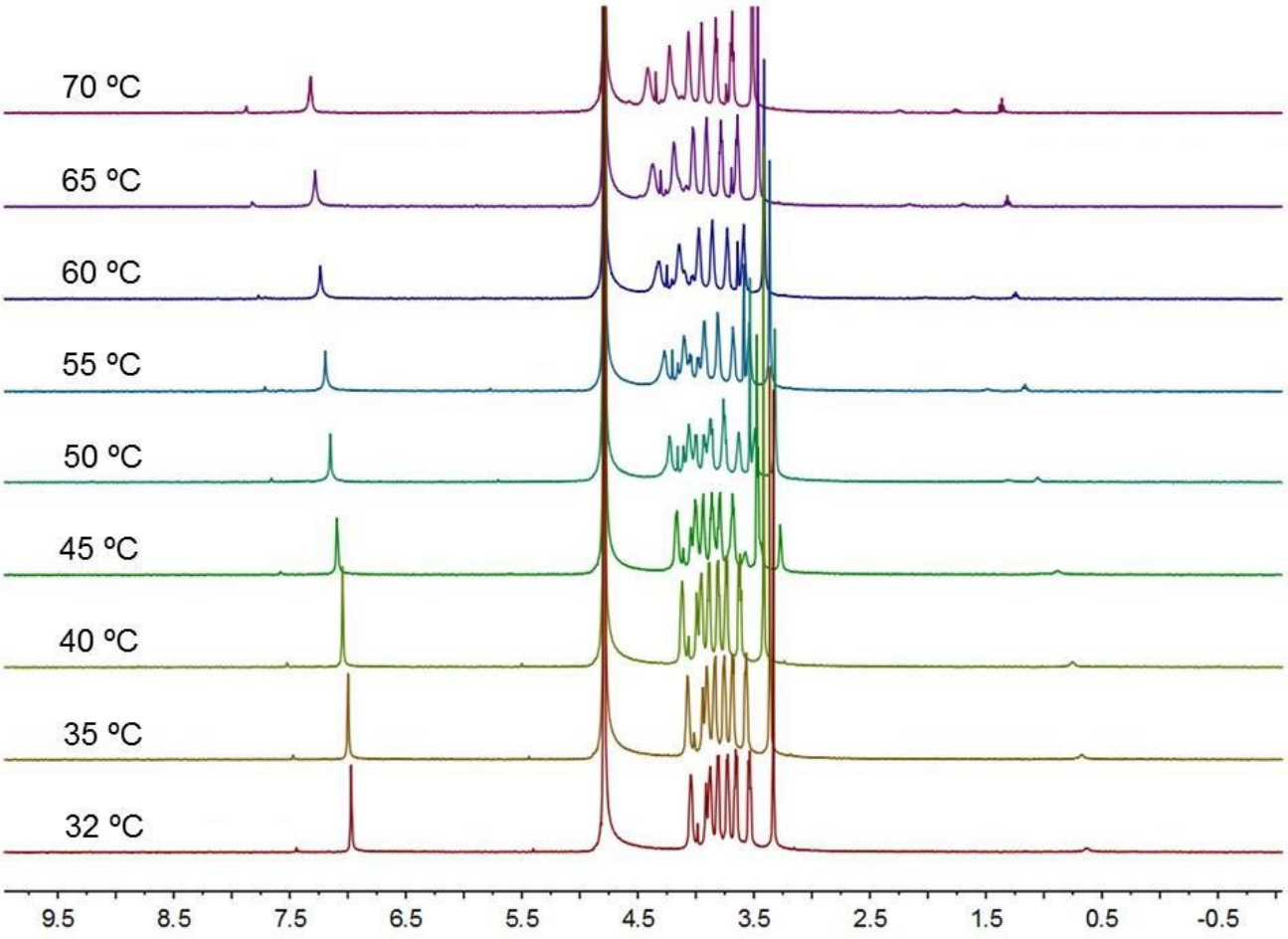

Figure S40. Variable-temperature ^{1}H NMR spectra (400 MHz) of **P5** and **G4** (2.00 mM) in D_2O.

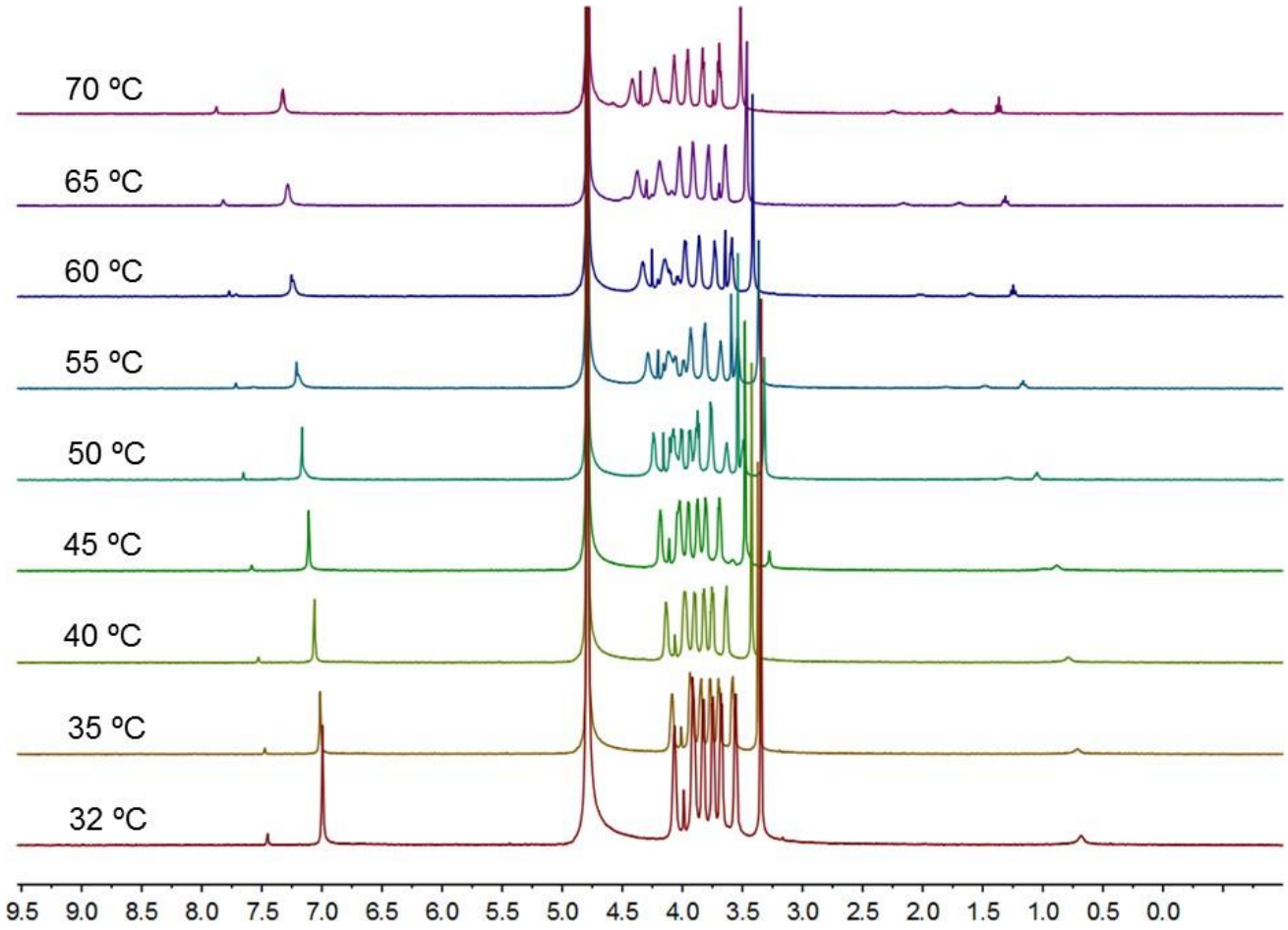

Figure S41. Variable-temperature ^{1}H NMR spectra (400 MHz) of **P5** and **G5** (2.00 mM) in D_2O.

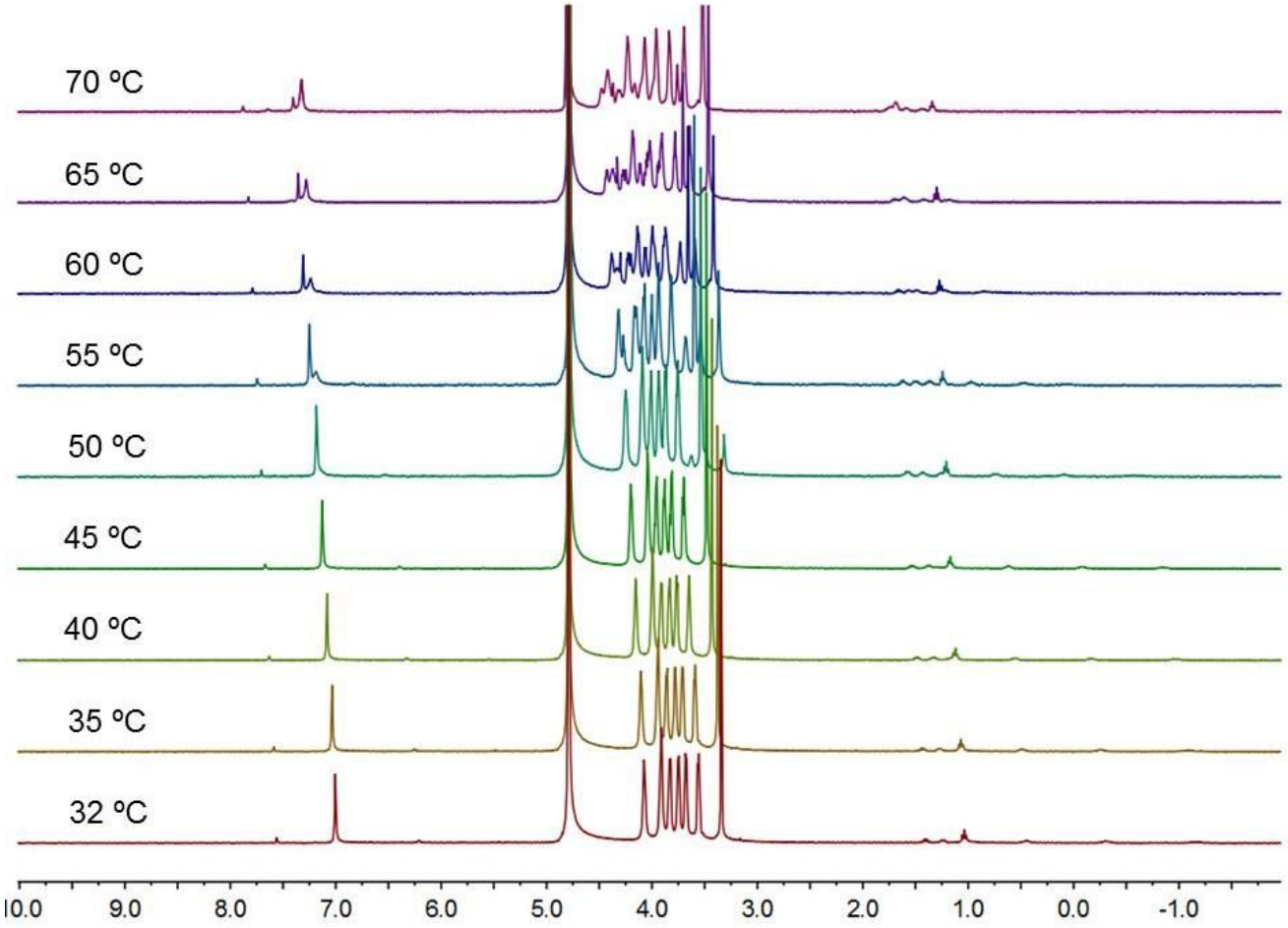

Figure S42. Variable-temperature ^{1}H NMR spectra (400 MHz) of **P5** and **G6** (2.00 mM) in D_2O.

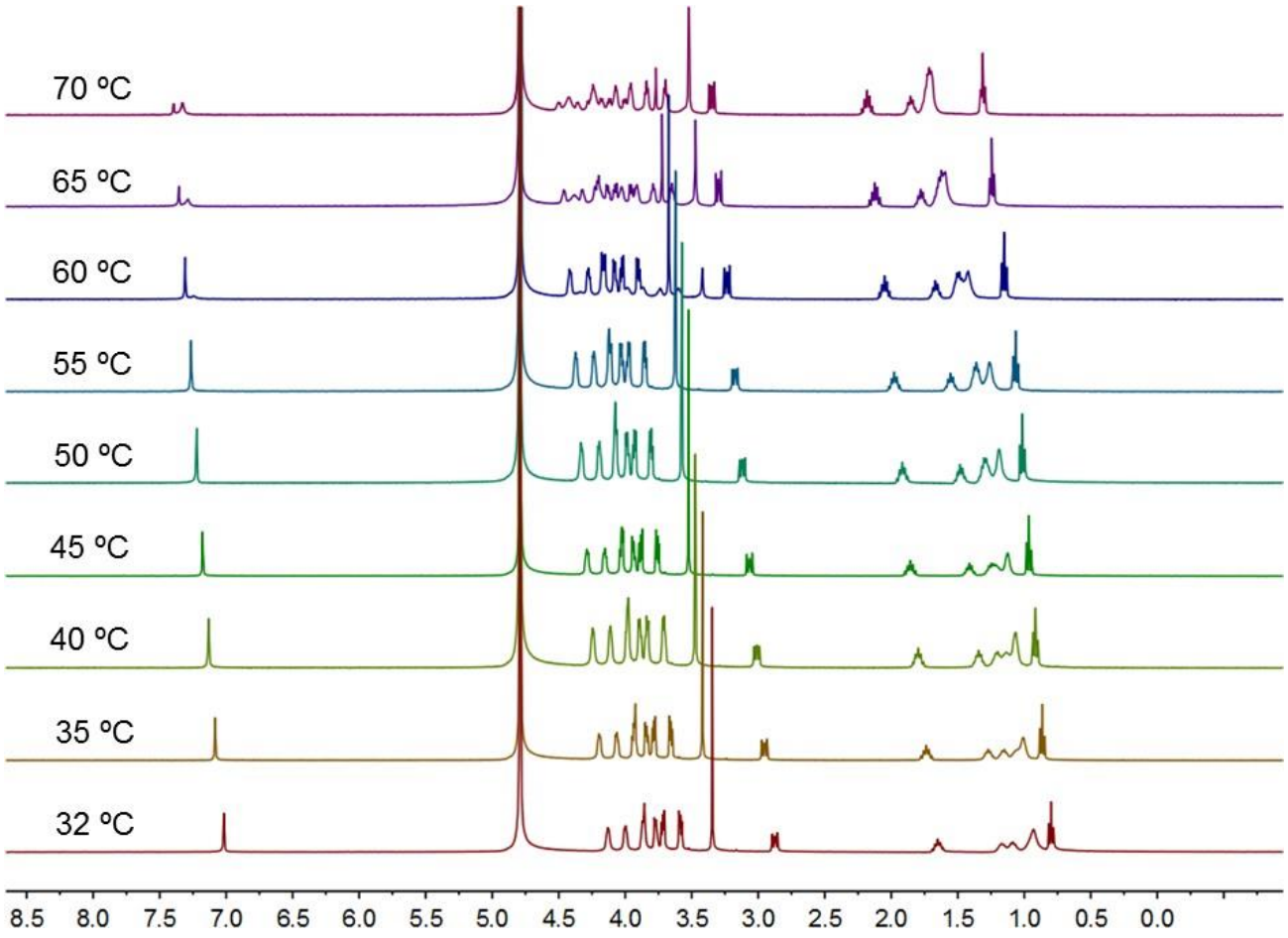

Figure S43. Variable-temperature ^{1}H NMR spectra (400 MHz) of **P5** and **G9** (2.00 mM) in D_2O.

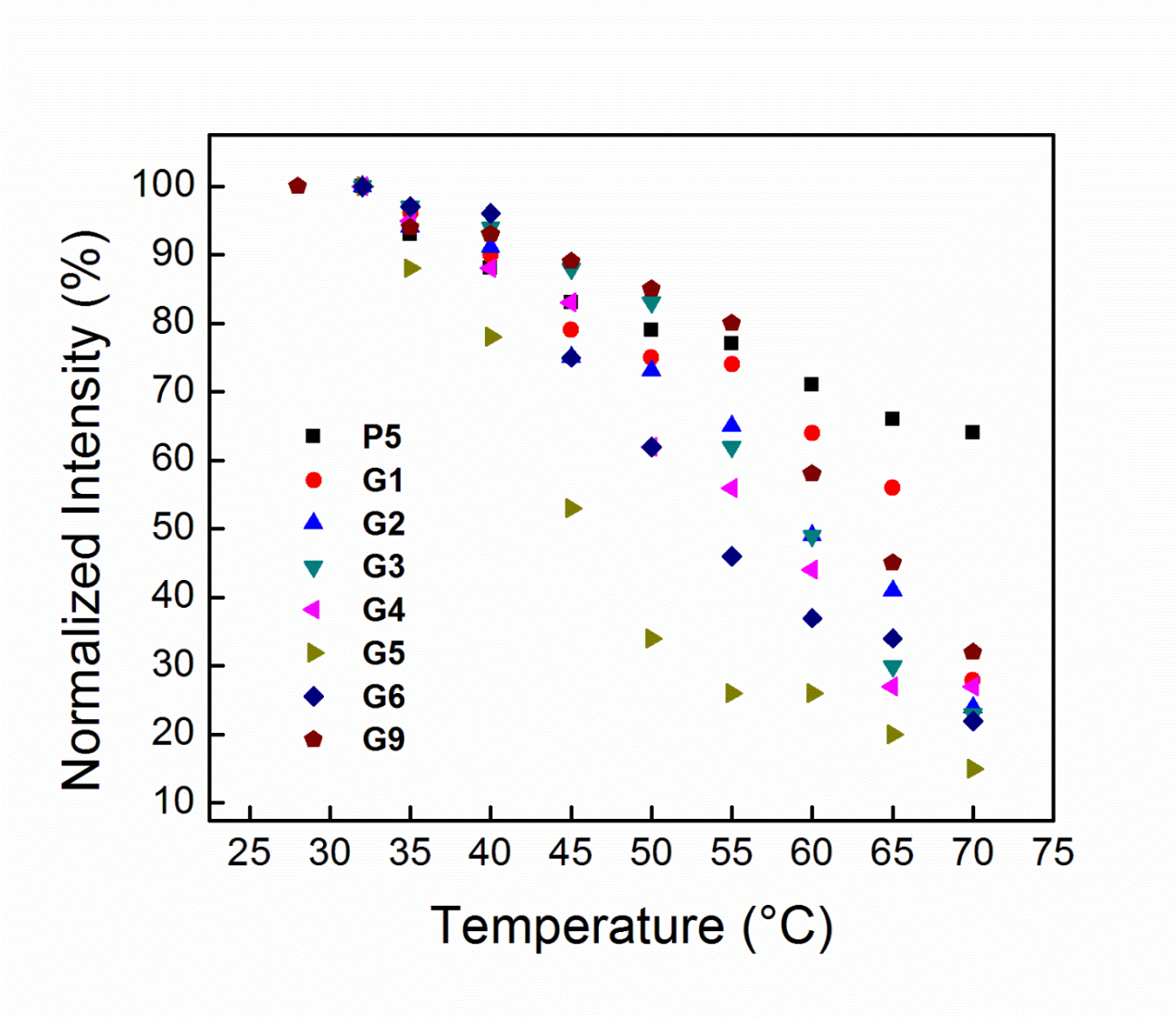

Figure S44. Temperature dependence of normalized intensity for **P5** upon addition of guests.

6. 2D NOESY spectra of equimolar mixture of **P5** and **G** in D_2O

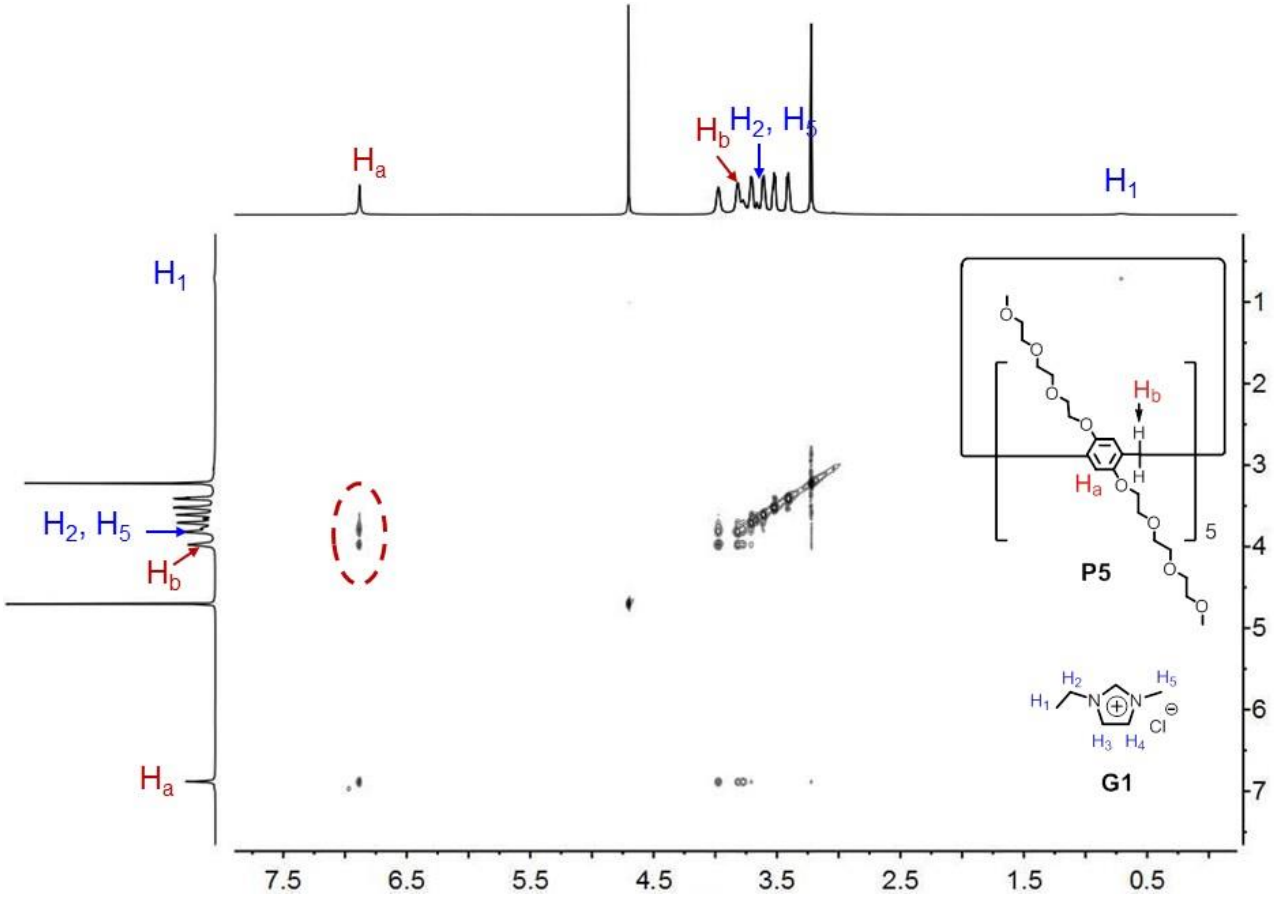

Figure S45. 2D ^{1}H-^{1}H NOESY spectrum of **P5⊃G1** (400 MHz, room temperature, D_2O). [**P5**] = 30.0 mM. [**G1**] = 30.0 mM.

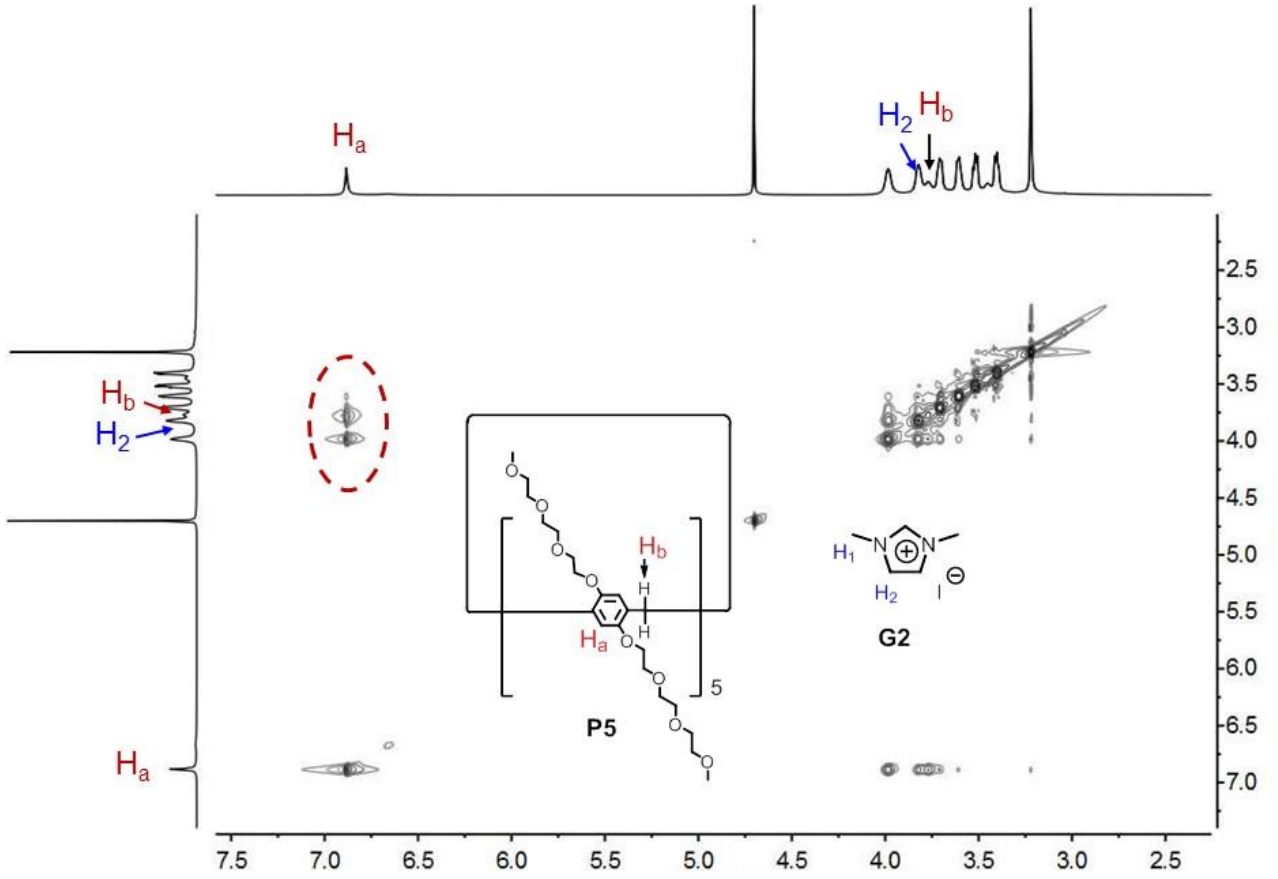

Figure S46. 2D ^{1}H-^{1}H NOESY spectrum of **P5⊃G2** (400 MHz, room temperature, D_2O). [**P5**] = 30.0 mM. [**G2**] = 30.0 mM.

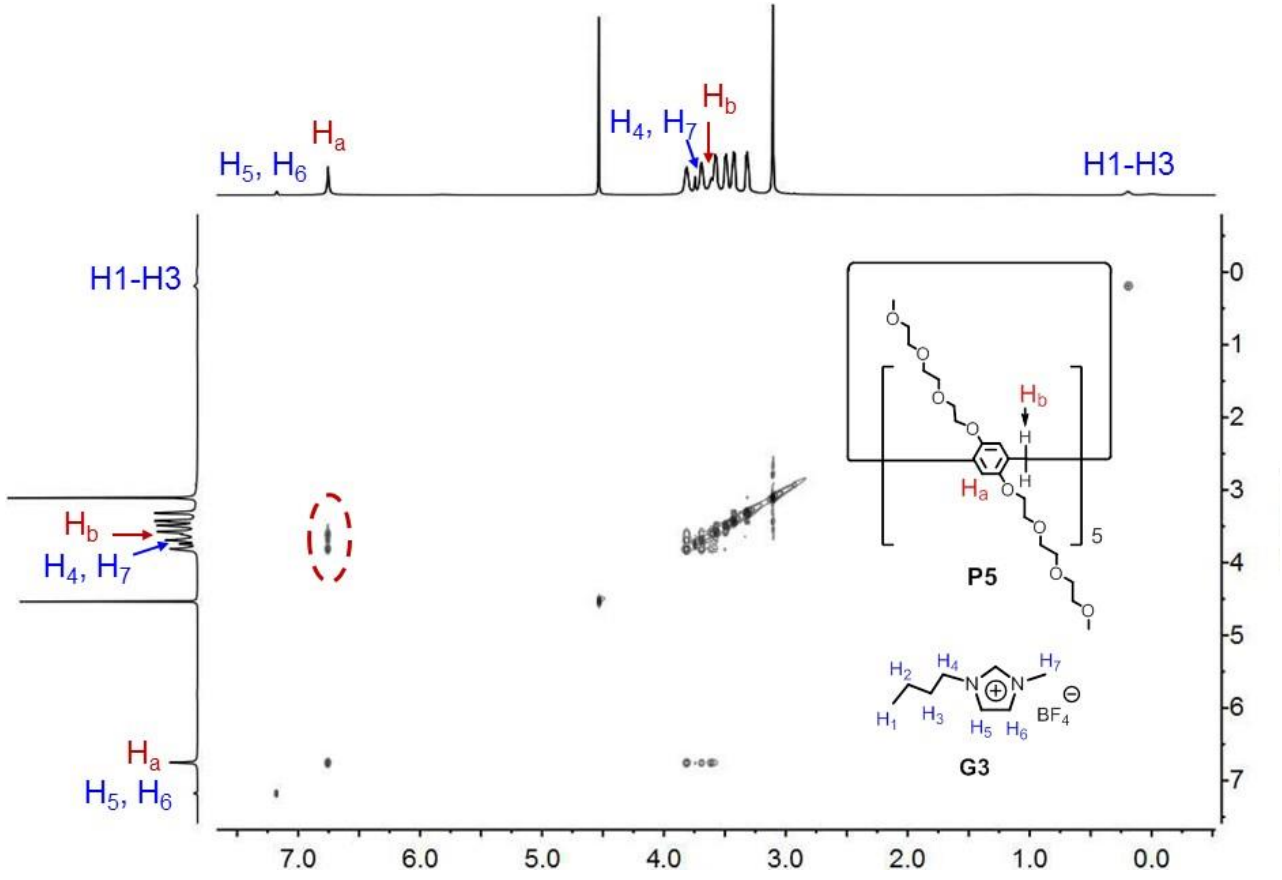

Figure S47. 2D ^{1}H-^{1}H NOESY spectrum of **P5⊃G3** (400 MHz, room temperature, D_2O). [**P5**] = 30.0 mM. [**G3**] = 30.0 mM.

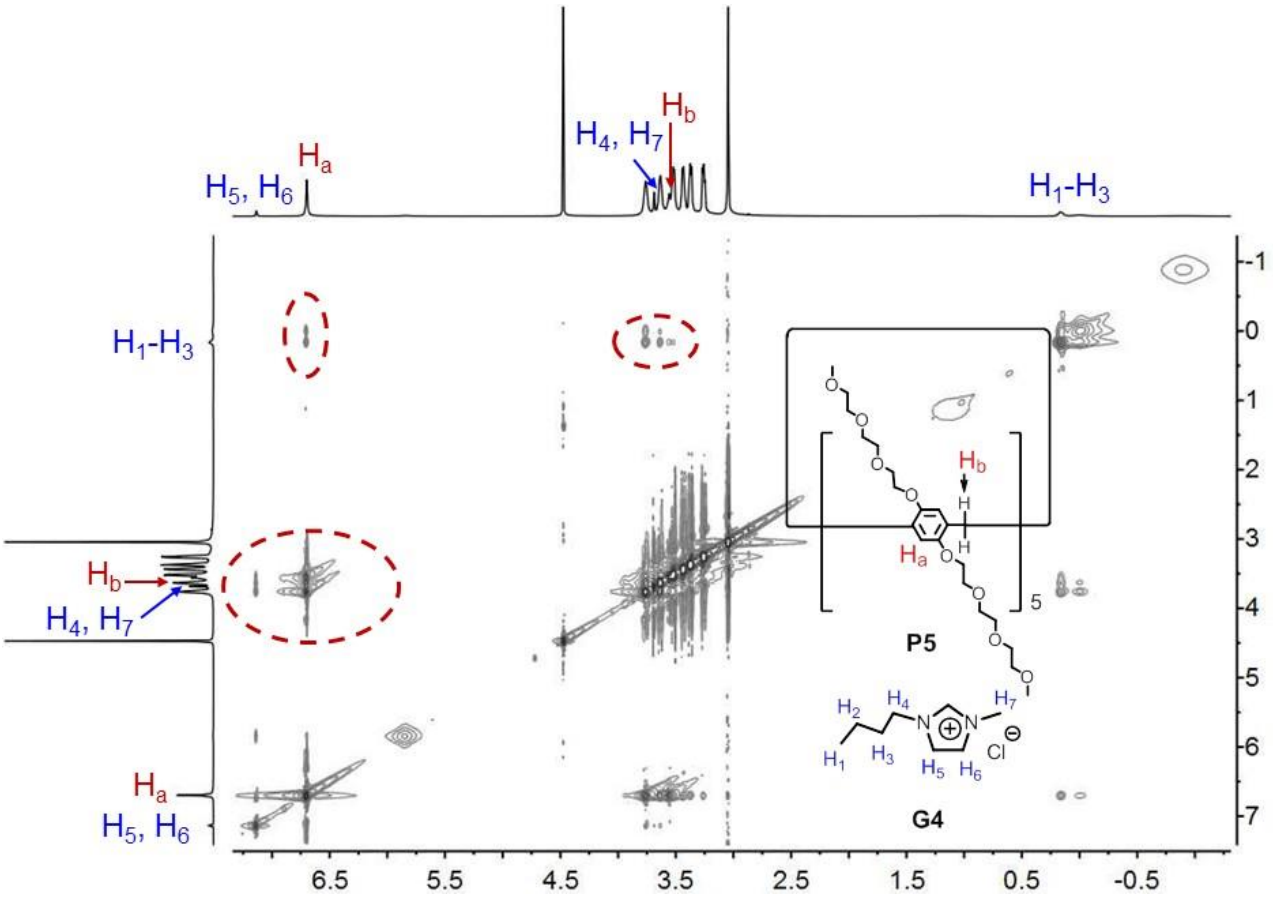

Figure S48. 2D ^{1}H-^{1}H NOESY spectrum of **P5⊃G4** (400 MHz, room temperature, D_2O). [**P5**] = 30.0 mM. [**G4**] = 30.0 mM.

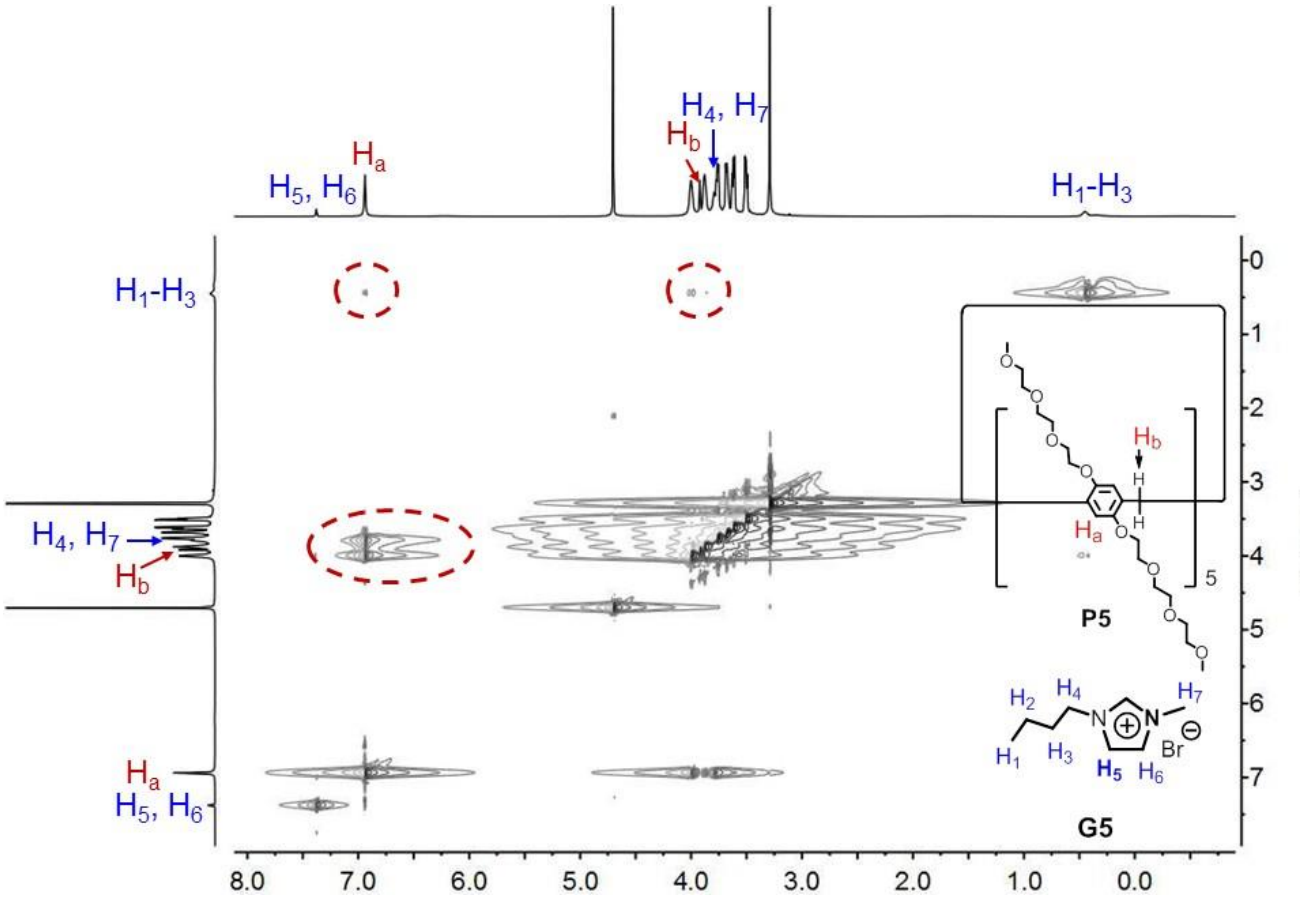

Figure S49. 2D ^{1}H-^{1}H NOESY spectrum of **P5⊃G5** (400 MHz, room temperature, D_2O). [**P5**] = 30.0 mM. [**G5**] = 30.0 mM.

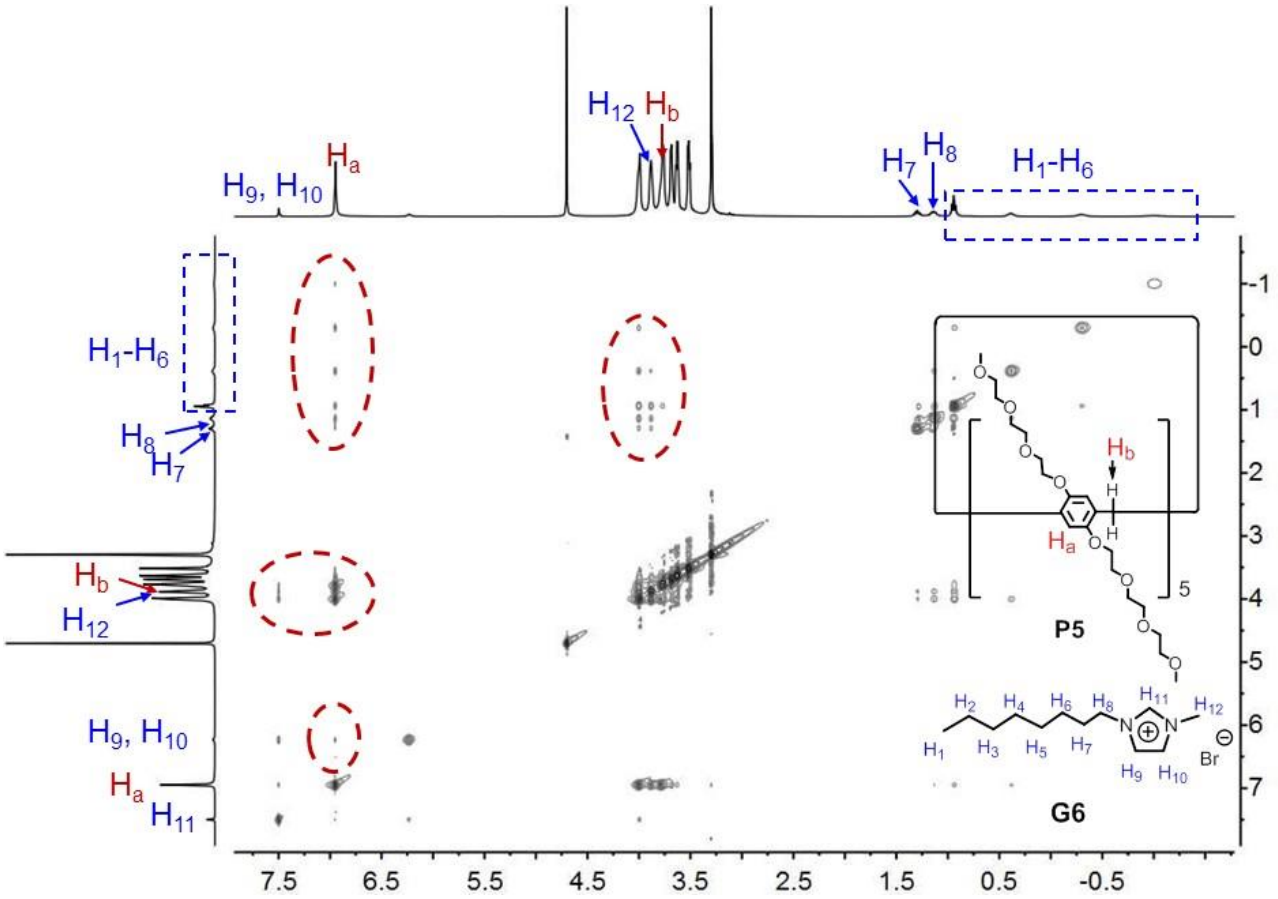

Figure S50. 2D ^{1}H-^{1}H NOESY spectrum of **P5⊃G6** (400 MHz, room temperature, D_2O). [**P5**] = 30.0 mM. [**G6**] = 30.0 mM.

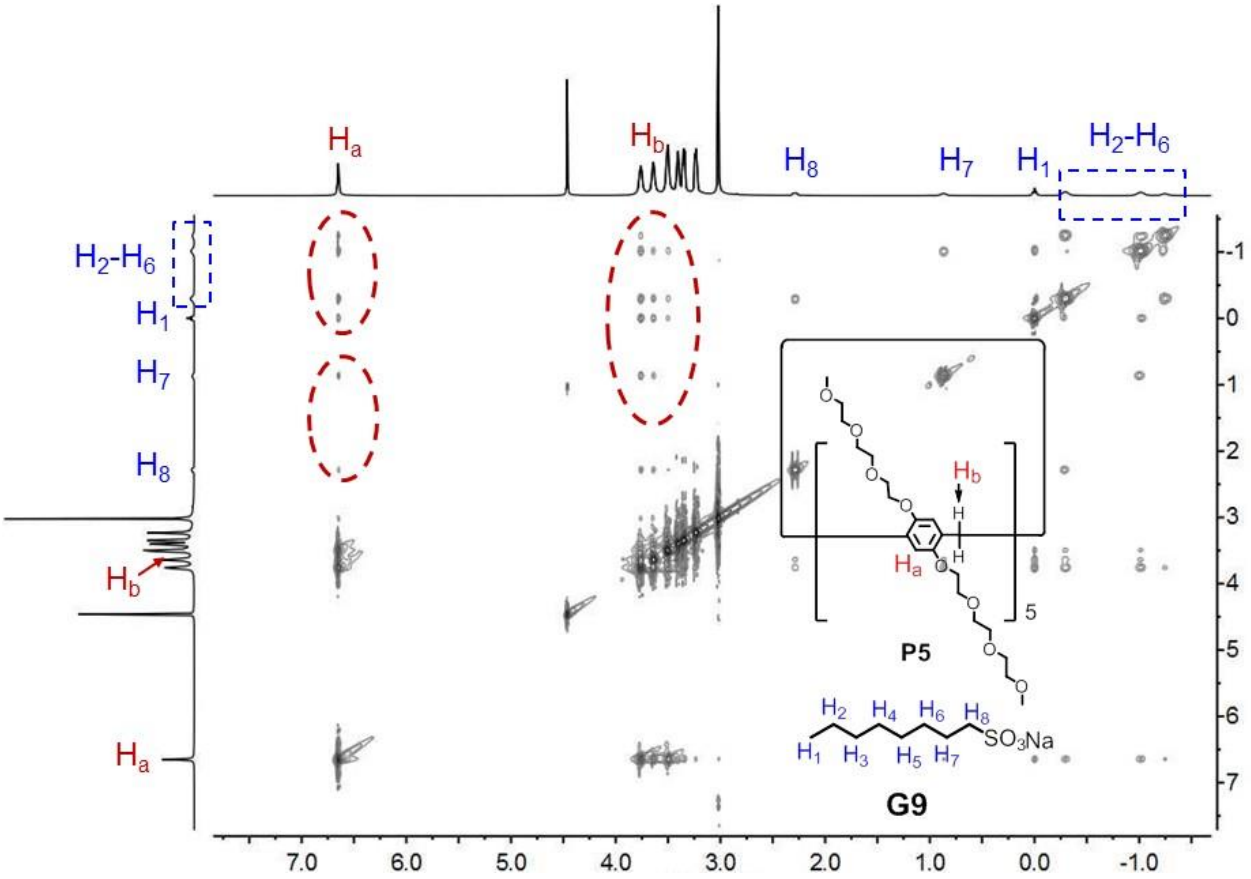

Figure S51. 2D ^{1}H-^{1}H NOESY spectrum of **P5⊃G9** (400 MHz, room temperature, D_2O). [**P5**] = 30.0 mM. [**G9**] = 30.0 mM.

7. T_{cloud} of supramolecular pairs by UV/Vis measurements

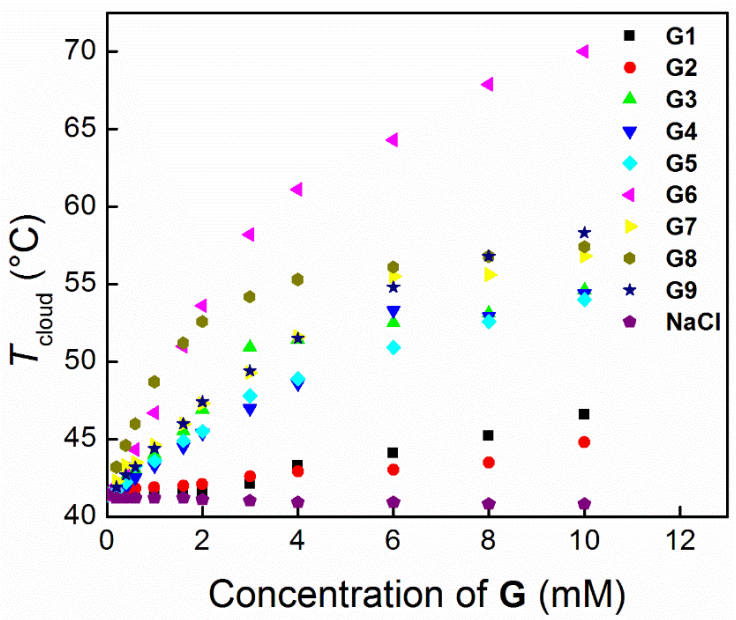

Figure S52. T_{cloud} of host-guest complexes.

References:

S1. T. Ogoshi, R. Shiga, and T. Yamagishi, *J. Am. Chem. Soc*., 2012, **134**, 4577−4580.

S2. K. A. Connors, *Binding Constants*; Wiley: New York, 1987; P. S. Corbin, Ph.D. Dissertation,University of Illinois at Urbana-Champaign, Urbana, IL, 1999; P. R. Ashton, R. Ballardini, V. Balzani, M. Belohradsky, M. T. Gandolfi, D. Philp, L. Prodi, F. M. Raymo, M. V. Reddington, N. Spencer, J. F. Stoddart, M. Venturi and D. J. Williams, *J. Am. Chem. Soc.*, 1996, **118**, 4931−4951.